

**DETECTION OF DC INJECTION AND MEASURING AC CURRENT  
WITH A SINGLE SYSTEM FOR  
ELECTRIC VEHICLE CHARGING AND DISCHARGING**

by

Olga Mironenko

A dissertation submitted to the Faculty of the University of Delaware in partial fulfillment of the requirements for the degree of Doctor of Philosophy in Electrical and Computer Engineering

Summer 2020

© 2020 Olga Mironenko  
All Rights Reserved

**DETECTION OF DC INJECTION AND MEASURING AC CURRENT  
WITH A SINGLE SYSTEM FOR  
ELECTRIC VEHICLE CHARGING AND DISCHARGING**

by

Olga Mironenko

Approved: \_\_\_\_\_  
Kenneth E. Barner, Ph.D.  
Chair of the Department of Electrical and Computer Engineering

Approved: \_\_\_\_\_  
Levi T. Thompson, Ph.D.  
Dean of the College of Engineering

Approved: \_\_\_\_\_  
Douglas J. Doren, Ph.D.  
Interim Vice Provost for Graduate and Professional Education and  
Dean of the Graduate College

I certify that I have read this dissertation and that in my opinion it meets the academic and professional standard required by the University as a dissertation for the degree of Doctor of Philosophy.

Signed: \_\_\_\_\_

Willett Kempton, Ph.D.  
Professor in charge of dissertation

I certify that I have read this dissertation and that in my opinion it meets the academic and professional standard required by the University as a dissertation for the degree of Doctor of Philosophy.

Signed: \_\_\_\_\_

Fouad Kiamilev, Ph.D.  
Member of dissertation committee

I certify that I have read this dissertation and that in my opinion it meets the academic and professional standard required by the University as a dissertation for the degree of Doctor of Philosophy.

Signed: \_\_\_\_\_

Chase Cotton, Ph.D.  
Member of dissertation committee

I certify that I have read this dissertation and that in my opinion it meets the academic and professional standard required by the University as a dissertation for the degree of Doctor of Philosophy.

Signed: \_\_\_\_\_

Gregory Poilasne, Ph.D.  
Member of dissertation committee

## ACKNOWLEDGEMENTS

First of all, I would like to thank NRG Energy and Nuvve Corp. for the research funding.

Next, I would like to thank my Ph.D. advisors: Prof. Willett Kempton and Prof. Fouad Kiamilev. My Ph.D. work would not have been done without their valuable advice and support. I really appreciate their guidance and encouragement not only about the academic topics but also about career and life decisions. I am truly grateful for their belief in me even when I didn't believe in myself. Prof. Kempton and Prof. Kiamilev made my Ph.D. journey very exciting, inspiring and unforgettable.

I would also like to thank Prof. Chase Cotton for his help and great advice how to prepare for a job interview.

I would like to thank my colleagues and friends at V2G and CVORG groups. They are very knowledgeable and just great people to work with. Special thanks to Garrett Ejzak, Rodney McGee, Josh Marks and Andrea Wait for their precious design advice and help. They are excellent engineers and great friends.

Personally, I would like to thank my husband and my best friend Alexander Mironenko for his love, support and motivation. He was always there to share my successes and my failures. I would also like to thank my parents Elena and Mikhail Zakharov for their love, encouragement, belief and motivation to never give up. Also, I would like to thank my brother Aleksei Zakharov who emotionally supported me throughout these challenging years.

Finally, I would like to thank my closest friends for their friendship and moral support: Yulia Karymova, Olga Arshinova, Tianne Lassiter, Teddy Katayama, Abhishek Joshi and Miguel Hernandez.

## TABLE OF CONTENTS

<b>LIST OF TABLES</b> . . . . .	<b>viii</b>
<b>LIST OF FIGURES</b> . . . . .	<b>ix</b>
<b>ABSTRACT</b> . . . . .	<b>x</b>
 <b>Chapter</b>	
<b>1 INTRODUCTION</b> . . . . .	<b>1</b>
1.1 Introduction . . . . .	1
<b>REFERENCES</b> . . . . .	<b>3</b>
 <b>2 CURRENT SENSING TECHNIQUES FOR REVENUE METERING AND DETECTION OF DIRECT CURRENT INJECTION FROM ELECTRIC VEHICLES: A REVIEW</b> . . . . .	 <b>4</b>
2.1 Abstract . . . . .	4
2.2 Introduction . . . . .	5
2.3 Review of current sensing techniques . . . . .	7
2.3.1 Shunt . . . . .	8
2.3.2 Current Transformer . . . . .	8
2.3.3 Rogowski Coil . . . . .	9
2.3.4 Hall Effect Sensor . . . . .	10
2.3.4.1 Open-Loop Hall Effect Sensor . . . . .	11
2.3.4.2 Closed-Loop Hall Effect Sensor . . . . .	12
2.3.5 Fluxgate Sensor . . . . .	13
2.3.6 Magneto Resistance Effect Sensors . . . . .	15
2.3.6.1 Anisotropic Magneto Resistance Sensors . . . . .	15
2.3.6.2 Giant Magneto Resistance Sensors . . . . .	17

2.3.6.3	Tunneling Magneto Resistance Sensors . . . . .	18
2.4	Possible solutions . . . . .	19
2.5	Conclusions . . . . .	20
2.6	Acknowledgement . . . . .	21
<b>REFERENCES . . . . .</b>		<b>22</b>
<b>3</b>	<b>INTEGRATED ELECTRIC VEHICLE SHUNT CURRENT SENSING SYSTEM FOR CONCURRENT REVENUE METERING AND DETECTION OF DC INJECTION . . . . .</b>	<b>28</b>
3.1	Abstract . . . . .	28
3.2	Introduction . . . . .	29
3.3	Prototype Design . . . . .	31
3.3.1	System Requirements . . . . .	31
3.3.2	Selecting the Current Sensor . . . . .	32
3.3.3	Shunt current sensor operating principle . . . . .	33
3.3.4	Design Challenges . . . . .	33
3.3.4.1	Single Sensor for AC and DC Measurements . . . . .	33
3.3.4.2	High-Side Current Sensing . . . . .	34
3.3.4.3	Power Dissipation and Energy Losses . . . . .	35
3.3.5	Power and Energy Losses due to the Shunt . . . . .	35
3.3.6	Prototype System Components . . . . .	35
3.4	Prototype Validation . . . . .	38
3.4.1	Accuracy of AC current measurements . . . . .	38
3.4.2	DC Injection Detection . . . . .	40
3.4.2.1	Accuracy of DC injection detection . . . . .	40
3.4.2.2	Effect of large AC current on DC injection detection . . . . .	42
3.4.3	Prototype System Cost-Effectiveness . . . . .	42
3.5	Conclusions . . . . .	43
3.6	Future Work . . . . .	44
3.7	Acknowledgement . . . . .	44
<b>REFERENCES . . . . .</b>		<b>45</b>

<b>4</b>	<b>COMPARING DEVICES FOR CONCURRENT MEASUREMENT OF AC CURRENT AND DC INJECTION FOR ELECTRIC VEHICLE CHARGING . . . . .</b>	<b>48</b>
4.1	Abstract . . . . .	48
4.2	Introduction . . . . .	49
4.3	Current Transformer Current Sensing System . . . . .	51
4.3.1	Operating principle . . . . .	51
4.3.2	System structure and capabilities . . . . .	52
4.3.3	Accuracy . . . . .	53
4.3.4	Cost . . . . .	53
4.4	Shunt Current Sensing System . . . . .	54
4.4.1	Operating principle . . . . .	54
4.4.2	System structure and capabilities . . . . .	54
4.4.3	Accuracy . . . . .	56
4.4.4	Cost . . . . .	56
4.5	Fluxgate Current Sensing System . . . . .	57
4.5.1	Operating principle . . . . .	57
4.5.2	System structure and capabilities . . . . .	57
4.5.3	Accuracy . . . . .	58
4.5.4	Cost . . . . .	58
4.6	Systems comparison and recommended applications . . . . .	59
4.7	Conclusions . . . . .	60
4.8	Acknowledgement . . . . .	60
	<b>REFERENCES . . . . .</b>	<b>61</b>
	<b>CONCLUSIONS . . . . .</b>	<b>64</b>

## LIST OF TABLES

2.1	Today's EVSE current sensor versus required current sensor characteristics. . . . .	6
2.2	Comparison of potential current sensors for EVSE application. . . .	19
3.1	The current sensing system requirements for bidirectional EVSEs. . .	31
3.2	Main design parts specification. . . . .	38
3.3	AC current measurements for charging and discharging. . . . .	39
3.4	Systems cost comparison for single-phase EVSE. . . . .	42
4.1	Current metering system requirements for single-phase and for three-phase EVSEs. . . . .	50
4.2	Current transformer current sensing system: detailed cost for single and three-phase EVSE. Hall-Effect LEM sensor is added only for DC injection detection price estimate. . . . .	53
4.3	Shunt current sensing system: detailed cost for single and three-phase EVSE. . . . .	56
4.4	Fluxgate current sensing system: detailed cost for single and three-phase EVSE . . . . .	59
4.5	Comparison of three current sensing systems for single-phase and three-phase EVSEs . . . . .	59

## LIST OF FIGURES

2.1	Air-core Rogowski Coil with integrator. . . . .	9
2.2	Hall Effect principle: (a) No magnetic field is present. (b) Presence of perpendicular magnetic field B. . . . .	11
2.3	Operating principle of Open-Loop Hall Effect current sensor. . . . .	12
2.4	Basic fluxgate sensor. . . . .	13
2.5	The Vacquier fluxgate sensor. . . . .	14
2.6	An AMR sensor with barber poles. . . . .	16
2.7	F.W Bell AMR current sensor. . . . .	17
2.8	Spin-valve GMR sensor: (a) No external magnetic field. (b) External magnetic field parallel to pinned ferromagnetic layer. (c) External magnetic field antiparallel to pinned ferromagnetic layer. . . . .	18
3.1	Current sensing single phase system block diagram. . . . .	36
3.2	Setting the DC injection alarm threshold for positive (right line) and negative (left line) DC injection. . . . .	40
3.3	Non-linearity error (% of full scale). . . . .	41
4.1	Current transformer current sensing system for a single-phase EVSE	52
4.2	Current sensing single phase system block diagram. . . . .	55
4.3	Fluxgate current sensing system's prototype: (a) The sensor head. (b) Controller board (images used by permission of Magnetic Sensor Systems, LLC). . . . .	58

## ABSTRACT

Modern power systems increasingly include distributed generation and storage. In addition to solar, these include newer technologies such as the Vehicle-to-Grid (V2G) technology, where energy, stored in electric vehicle (EV) batteries, is injected back to the AC grid when there is a need. Injected power is regulated by many standards and laws, with electrical requirements including anti-islanding, limitation of harmonics, low-voltage ride-through, fault current and DC injection. For solar and battery storage, including V2G, the power to the grid is provided by a power converter taking DC from the solar panels or battery, converting to AC, and injecting AC power onto the grid. This thesis addresses the problem of accurate measurement of AC power, while using the same device to detect DC injection. Any faulty or improperly designed power converter can inject DC into the AC grid, but the high power converters of electric vehicles represent a particular concern. DC injection may cause saturation of transformer cores, overheating of grid-connected equipment, and acceleration of cable corrosion. Therefore, it is important to ensure that its value stays within the allowable limit stated in the "Limitation of DC injection" in the IEEE 1547-2018 standard. Although the power converter is responsible for limiting DC on the AC lines, additional verification of DC injection by the Electric Vehicle Supply Equipment (EVSE) would be a cost-effective extra safety measure, allowing diverse EVs to be checked by one EVSE. Importantly, a V2G-capable EVSE must be able to carry out concurrent high-precision AC and moderate-precision DC current measurements to fulfill revenue metering requirements in the most economical way.

In the first part of the work, we will review the DC injection problem and commonly used current sensing techniques to evaluate the most promising current-sensor candidates. In the second part of this work, we will present an Integrated Shunt Current

Sensing System that we have designed, prototyped, and validated. The design accomplishes cost-effective AC current measurements within 1.0 accuracy class required for revenue metering. In addition, the prototype is able to simultaneously detect DC injection of  $\geq 400$  mA in AC current up to 80 A in accordance with the "Limitation of DC injection" section in IEEE 1547-2018 standard. Positive DC injection detection accuracy at the limit value of 400 mA is 8.25%. Negative DC injection detection accuracy is 16.5%. We will discuss system design challenges, test results, and the cost analysis. In the third and final part of the work, we will review alternative solutions and recommend an optimal solution for the concurrent measurement of the AC current and DC injection to be used for EV charging and discharging.

# Chapter 1

## INTRODUCTION

### 1.1 Introduction

The work presented in the dissertation consists of 3 studies. Chapter 2 describes the first study introducing the DC injection problem, its historical roots as well as explains Distributed Energy Resources (DER) interconnection standards. Next, we describe Vehicle-to-Grid technology (V2G) and how DC injection problem is related to V2G and EV charging in general. Further, we provide a motivation to design a new cost-effective current sensing system for electric vehicle supply equipment (EVSE) capable of DC injection detection and high precision AC current measurement. Finally, we review commonly used current sensing techniques to select the most promising candidates for next research steps.

After reviewing eight current sensing technologies in Chapter 2, the shunt was selected from the list of suitable sensors as the simplest and inexpensive solution. Chapter 3 introduces the second study namely current sensing system we designed, prototyped and validated based on the integrated shunt. First, we introduce the problem's background and the sensing system design requirements. Next, we explain the operating principle of the shunt, its advantages and drawbacks as well as a motivation behind the sensor selection. Next, we list the design challenges and concerns such as the system power dissipation and energy losses due to the shunt. After that we introduce the prototype components as well as the design to integrate the prototype into a single and three phase EVSE. Further, we demonstrate the prototype's validation. The results include the accuracy of AC current measurements for charging and discharging, ability to detect DC injection of  $\geq 400$  mA in a presence of AC currents up to 80 A,

and DC injection detection accuracy at the limit value. Finally, we demonstrate the cost-effectiveness of the designed system over today's common practice of a current transducer (CT).

Chapter 4 represents the third study where we compare performance and cost of the system designed in chapter 3 with the current sensing system (CT) commonly used in EVSE as well as with other top candidate namely the fluxgate current sensor. First, we introduce the structure, capabilities and limitations of each system. Further, we provide the accuracy and the cost of each system under interest. Finally, we compare the systems based on capabilities to measure both AC current up to 80 A with high precision and detect the DC injection of  $\geq 400$  mA along with the cost of each system. In conclusion, we provide a recommendation for the optimal solution to be used in bidirectional 19.2 kW single-phase EVSEs.

The chapters 2, 3, 4 consist of three papers [3], [1], and [2] respectively. The first paper is submitted for review to *SAE International Journal of Electrified Vehicles*, the second paper is re-submitted to *IEEE Transactions on Instrumentation and Measurement* and the third paper is ready for submission to *World Electric Vehicle Journal*. Each of these three articles here is represented as one chapter, but with an additional one-page transition at the beginning of each, to make the dissertation more readable as a single document.

In addition, we conducted some research in collaboration with Magnetic Sensor Systems toward the integration of the fluxgate current sensing system, mentioned in chapter 4, into the application specific integration circuit (ASIC). Miniaturization of the circuit into an ASIC could significantly reduce the manufacturing cost of the sensor, the amount of necessary space inside the EVSE, and also potentially improve the accuracy of the system. However, after initial design steps the interest was shifted toward the shunt sensor as a less complicated and more promising solution.

## REFERENCES

- [1] Olga Mironenko, Garrett Ejzak, Willett Kempton, and Fouad Kiamilev. Integrated electric vehicle shunt current sensing system for concurrent revenue metering and detection of dc injection. *re-submitted to IEEE transactions on Instrumentation and Measurement*, June 2020.
- [2] Olga Mironenko, Willett Kempton, and Fouad Kiamilev. Comparing devices for concurrent measurement of ac current and dc injection for electric vehicle charging. *Ready for submission to World Electric Vehicle Journal*, June 2020.
- [3] Olga Mironenko, Willett Kempton, and Fouad Kiamilev. Current sensing techniques for revenue metering and detection of direct current injection from electric vehicles: A review. *submitted to SAE International Journal of Electrified Vehicles*, May 2020.

## Chapter 2

### CURRENT SENSING TECHNIQUES FOR REVENUE METERING AND DETECTION OF DIRECT CURRENT INJECTION FROM ELECTRIC VEHICLES: A REVIEW

*Chapter 2 describes the first study introducing the DC injection problem, its historical roots as well as explains Distributed Energy Resources (DER) interconnection standards. Next, we describe Vehicle-to-Grid technology (V2G) and how DC injection problem is related to V2G and EV charging in general. Further, we provide a motivation to design a new cost-effective current sensing system for electric vehicle supply equipment (EVSE) capable of DC injection detection and high precision AC current measurement. Finally, we review commonly used current sensing techniques to select the most promising candidates for next research steps.*

#### 2.1 Abstract

Contemporary power networks increasingly include distributed generation and storage, which must follow interconnection standards to ensure power quality and grid safety. One such standard is the "Limitation of DC injection" in the IEEE 1547-2018 standard. Any poorly designed or malfunctioning power converter can inject DC, but high power converters, such as used for electric vehicle (EV) chargers, are a proportionally larger concern. We propose that Electric Vehicle Supply Equipment (EVSE) be responsible for monitoring the DC injection level in AC current to and from EV on-board inverters to provide extra protection in case of on-board equipment failure. Another function of the EVSE is high precision AC current measurements for revenue metering. Due to mass production of EVSE, it is important to integrate DC injection detection into EVSE system cost-effectively. Therefore, it is advantageous for

AC current and DC injection to be measured with a single device. Due to inability of the most common revenue metering system to detect DC current, a new system with AC and DC measuring capabilities needs to be designed. The important design challenge is the large (two orders of magnitude) differences of measured AC vs. DC quantities on the same line. This paper introduces the DC injection problem in relation to EVs, and provides a review of commonly used current sensing techniques to evaluate the most promising candidates for the aforementioned system design.

## 2.2 Introduction

Modern power generation is moving from traditional centralized systems to distributed power systems such as supply equipment, energy storage, private generators, solar systems [18]. Many renewable energy sources (photovoltaic systems, fuel cells as well as battery storage systems) require DC/AC conversion to appropriately supply the standard AC frequency grid [13, 44]. In the past, inverters typically had a transformer located at the output for isolation purposes. This approach, however, has drawbacks including bulkiness, high cost and fair efficiency. Consequently, the research interest has shifted towards transformerless topology inverters. Without a transformer, however, there is a possibility of a small amount of DC current being injected onto the AC grid. This effect is referred to "DC injection". It deteriorates the power quality, may cause saturation of transformer cores, acceleration of cable corrosion and/or overheating of grid-connected equipment [18, 37]. According to the IEEE 1547-2018 standard, all systems connected with the utility electric power system (EPS) shall fulfill a set of requirements including the allowable level of DC injection, which is 0.5% of the full rated output current [6].

Storage capacities of EVs can be integrated into the power grid. When demand exceeds supply, EV batteries can be discharged to provide power to the grid, while an EV is parked and connected to an outlet. When supply exceeds demand, batteries can be charged to consume power for a short-term storage. The technology has been

developed at the University of Delaware, and is called Vehicle-to-Grid (V2G). In comparison with power plant generators, EV batteries enable a much more rapid response of electricity supply to changes in its demand. Although, automakers have been slow to add V2G capability due to its design complexity, commercial operations are beginning to be accepted [19].

Consequently, an EV, via electric vehicle supply equipment (EVSE), can be considered as DER equipment which can inject power back to the grid. Therefore, EV’s power electronics must follow DC Injection limitation rules, and pass any corresponding tests to obtain grid-connection approval [21, 41]. However, the connection safety is not fully guaranteed if the EV fails. We propose here that it should be the responsibility of the EVSE to verify an EV is adhering to these regulations at the point of connection. This is a cost-effective safety verification solution for DC monitoring in markets where such rules are in place, such as North America and Europe.

Another responsibility of an EVSE is to conduct high accuracy power and energy measurements for revenue metering. The accuracy criteria for revenue metering are described in NIST HB-44, ANSI C12.20 and IEC 62053-11 standards (0.5, 1.0 and 2.0 accuracy classes) [8, 3, 1]. Therefore, it is highly important to measure both AC current and DC injection, ideally with a single device to minimize the system cost. The challenges of a single sensor utilization are the large difference between AC and DC currents, and the high accuracy of AC readings across the entire range of 120A (see Table 2.1).

**Table 2.1:** Today’s EVSE current sensor versus required current sensor characteristics.

<b>Characteristics</b>	<b>BCT-013-200 CT</b>	<b>AC/DC CS</b>
DC detection	no	yes
AC current accuracy	$\pm 0.1\%$	$\leq \pm 0.5\%$
AC current range	200 A	$\geq 120\text{A}$
Thermal stability	good	good
Cost,\$	Medium	Lowest possible

The DC injection problem has been historically associated with grid-connected solar systems, and other distributed power sources requiring a DC/AC inverter. There are, therefore, a number of existing methods of mitigating this undesirable DC component in the output of an AC inverter. For instance, research presented in [12], proposes the DC offset prevention approach by using auto-calibration technique with Hall-Effect DC link current sensors. In addition, ref. [42] suggest the signal processing for DC current detection by obtaining frequency and phase information from the inverter software, and filtering the DC component for further suppression. Another DC injection control technique proposed by [11] employs a 1:1 coupled inductor and small range fluxgate current sensor (CS) for DC component extraction and the adjustment the inverter to minimize the injection. Although, the aforementioned methods demonstrated promising results, they are realized by power converter and included into its design. Therefore, they are not suitable for EVSE application since the EVSE doesn't have an inverter on-board and serves as a gateway between the grid and variety of EVs. On the other hand, the most common, revenue-grade AC current detection system uses a current transducer (CT), consisting of an induction coil surrounding the current-carrying conductor that converts current to voltage. For example, inside the University of Delaware EVSE, AC current is detected by BCT-013-200 Current Transformer and processed by a standard metrology chip. However, DC injection currents cannot be detected by this device, because DC cannot be detected by electromagnetic induction. For better understanding the future system requirements, a comparison between this sensor's capabilities and those which would be ideally desired is provided in Table 2.1.

### 2.3 Review of current sensing techniques

Due to a wide range of current sensing techniques available on the market nowadays, we present a comprehensive analysis to identify those options that would satisfy the system requirements. This study is focused on basic fundamentals, operating principles and key characteristics of the sensors. We analyze the existing commercially

available current sensing technologies potentially suitable for application in EVSE such as shunts, Rogowski coils, current transformers, Hall effect sensors, fluxgate sensors, and magneto-resistance effect sensors.

### **2.3.1 Shunt**

One of the popular current sensing techniques is shunt resistors due to their low cost, simplicity, acceptable accuracy, and their ability to measure low-frequency AC and DC currents. The shunt operates based on Ohm's Law of Resistance. The Voltage drop across the shunt is proportional to current flow and can easily be measured. Shunts must be installed into the current conductive path, and thus they can introduce significant power losses. This limits the high current application of shunts.

The other potential issues with shunts include: heat generation due to power dissipation, lack of galvanic isolation, and a voltage drop on the order of a few microvolts requiring additional elements for isolation and amplification of the signal for further processing. This can increase the size and cost of the system.

One more important parameter of a shunt that theoretically can adversely influence the accuracy is the thermal coefficient of resistance (TCR) of the shunt material. Modern shunts, however, are manufactured from low thermal drift alloys ( $<20\text{ppm}/^\circ\text{C}$ ), that provide acceptable thermal stability in most cases. Precision shunts with tolerances of  $\pm 0.1\%$ ,  $\pm 0.25\%$ ,  $\pm 0.5\%$  can be found on the market [38, 43, 23].

### **2.3.2 Current Transformer**

The most common method of isolated current measurement is the so-called current transformer. The operating principle of current transformers (CT) is Faraday's Law of Induction, and is limited to alternating current measurements.

The primary and secondary winding are coupled together in such a way as the induced secondary current proportional to the current to be measured. The relationship is determined by ratio of turns of the primary and secondary winding. CTs utilize magnetic core materials such as ferrite which serves as a magnetic flux concentrator

and enables higher accuracy of the device. CTs are a popular solution for power conversion applications due to their simplicity, high accuracy and output signal compatibility with analog-to-digital converter. However, the use of solid magnetic core materials, introduces core saturation in the event of high currents or in the presence of significant DC component, which negatively impacts the accuracy of the device. This issue can be mitigated by manufacturing magnetic cores from materials with high relative permeability. However, this increases the cost of the sensor [43, 20, 27].

### 2.3.3 Rogowski Coil

The Rogowski Coil's fundamental operating principle is similar to the CT's. The sensor also utilizes Faraday's Law of induction and can only measure AC current. This principle is illustrated in Fig. 2.1.

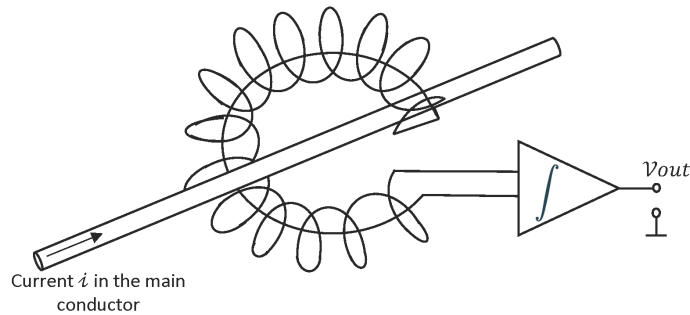


**Figure 2.1:** Air-core Rogowski Coil with integrator.

The coil essentially operates as an air core coil surrounding the main current carrying conductor. Alternating current generates oscillating magnetic flux which, in turn, induces a voltage in the Rogowski coil proportional to the time rate of change of current in the main conductor  $\frac{di(t)}{dt}$  and mutual inductance  $M$ :

$$v(t) = M \frac{di(t)}{dt} \quad (2.1)$$

Therefore, integration is required to derive an output signal proportional to the measured current:

$$i(t) = \frac{1}{M} \int v(t) dt \quad (2.2)$$

The integrator can be implemented with one of two approaches: analog or digital. The analog method requires high efficiency op-amps. In the digital approach the integrator is implemented as an Integrated Circuit by using MOSFETs.

Rogowski coils possess large current measurement capability, intrinsic isolation between the measured current and output signal, low cost, flexibility, high linearity, low temperature drift, and low power consumption. In addition, they don't display saturation and hysteresis issues as they do not use a magnetic core material. However, the sensitivity of Rogowski coils is low in comparison with CTs due to lack of high permeability magnetic core. In addition, commercially available Rogowski coils feature a low accuracy of approximately 1% [43, 29, 16].

### 2.3.4 Hall Effect Sensor

The Hall Effect Sensor is the first of a family of magnetic field based sensors. In contrast with Rogowski coils and CTs, magnetic field sensors can detect both static and dynamic fields and can, therefore, measure AC and DC currents. The current range of commercially available sensors is from 1 A to 5kA.

The Hall Effect, discovered by physicist Edwin Hall in 1879, says that a particle with charge  $Q$  moving inside magnetic field  $B$  with velocity  $V$ , will experience a force called the Lorentz force, which direction is perpendicular to both the velocity of the particle and the magnetic field [17, 23]:

$$F = Q(\mathbf{V} \times \mathbf{B}) \quad (2.3)$$

The effect of the force is the accumulation of conductive carriers at one edge of the conductor. Uneven distribution of the charge creates a potential difference which is proportional to magnetic field  $B$ . The Hall Effect is illustrated in Fig. 2.2.

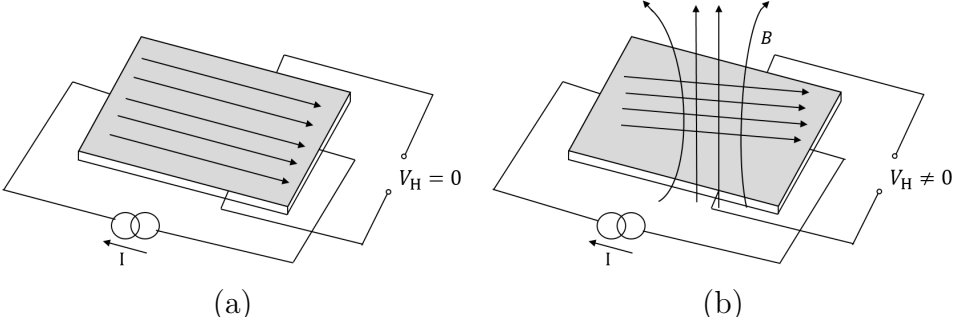


**Figure 2.2:** Hall Effect principle: (a) No magnetic field is present. (b) Presence of perpendicular magnetic field  $B$ .

In the absence of a magnetic field, the current distribution in a thin conductive sheet is homogeneous. Therefore, no potential difference is observed. However, if a perpendicular magnetic field  $B$  is applied, voltage occurs due to the current distortion. This voltage is proportional to the applied magnetic field and called the Hall voltage [2, 15, 9, 24].

There are two basic configurations of Hall Effect based current sensors : Open-Loop and Closed-Loop.

**2.3.4.1 Open-Loop Hall Effect Sensor**

The main operating principle of the Open-Loop current sensor is illustrated in Fig. 2.3.

The sensor consists of an air-gaped magnetic core with a Hall element installed in the gap surrounding the main current carrying conductor. The magnetic field  $B$  generated by primary current  $I_p$  is concentrated in this magnetic core, and is perpendicular to the Hall element. According to the Hall Effect, the magnetic field produces a distortion in the control current  $I_c$ , and generates a Hall voltage, which is proportional

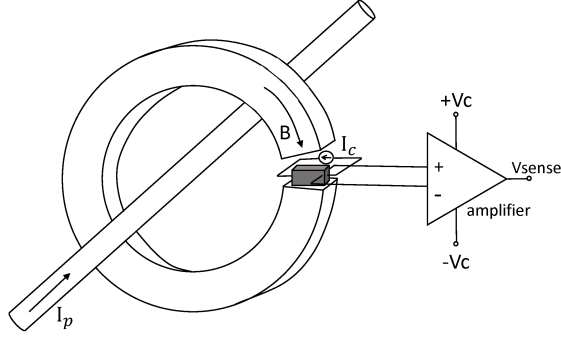


**Figure 2.3:** Operating principle of Open-Loop Hall Effect current sensor.

to the current in question. This signal must then be amplified to produce the desired signal output.

The open-loop configuration has a number of advantages such as simplicity, low cost, low power consumption and compactness. However, this configuration suffers from significant thermal drift. This configuration is also sensitive to external magnetic fields due to magnetic leakage within the core air gap. Achievable accuracy of Open-Loop Hall Effect sensors varies from  $\pm 0.5\%$  to  $\pm 2\%$ . In addition, Open-Loop sensors experience core losses due to hysteresis and eddy currents, which constrain the bandwidth of the sensing device [43, 23, 9, 34].

#### 2.3.4.2 Closed-Loop Hall Effect Sensor

In contrast with the Open-Loop configuration, in the Closed-Loop configuration the sensor uses the output signal as a compensation signal for the magnetization in the magnetic core. The output current is driven into a second winding to generate a secondary magnetic field which is opposite to that in the primary winding such that the net flux is zero.

This configuration significantly reduces the thermal drift of the sensor improving accuracy of the device to  $\pm 0.02\%$  -  $\pm 0.05\%$ . In addition, it eliminates losses due to

hysteresis and eddy currents. Moreover, Open-Loop current sensors introduce very good linearity and fast response times.

The major drawback of the technology is that it requires significant power to supply the compensation current. Besides that, the construction of the device is more complicated, expensive and bulky than a comparable open-loop sensor system [43, 25, 14, 23].

### 2.3.5 Fluxgate Sensor

Fluxgate sensors are one of the highest accuracy (up to  $\pm 0.0002\%$ ) magnetic sensors. They are exploited for DC or low-frequency AC magnetic fields measurements and current range of up to 500A. Fluxgate operates by exploiting the nonlinear dependency of ferromagnetic material permeability on the surrounding external magnetic field. The basic fluxgate sensor design is illustrated on in Fig. 2.4.

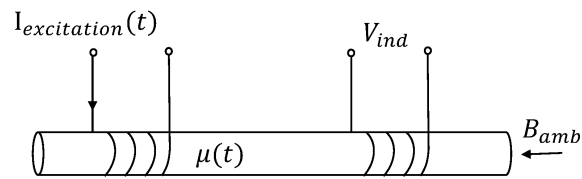


**Figure 2.4:** Basic fluxgate sensor.

The device topology consists of a ferromagnetic rod core, excitation coil, and pick up coil. A high frequency excitation current  $I_{excitation}(t)$  drives the core to saturation in both directions. In saturation, the magnetic permeability of the core material collapses causing a significant reduction in the DC ambient field magnetic flux. The pick up coil detects the voltage  $V_{ind}$  induced when the ambient magnetic flux collapse. The sense voltage signal will be the second harmonic of the excitation frequency. This

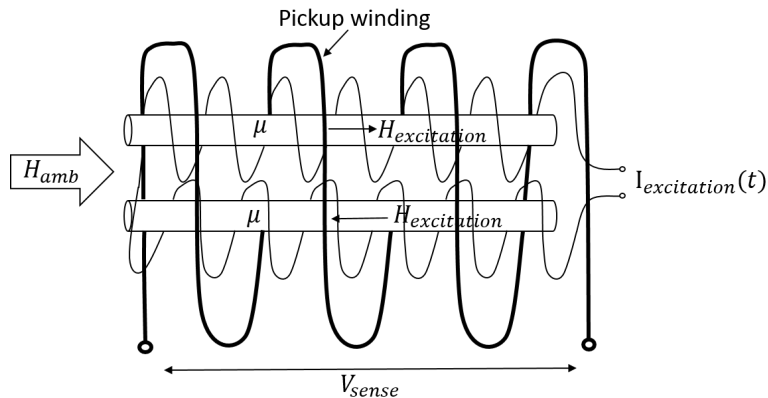


**Figure 2.5:** The Vacquier fluxgate sensor.

signal is proportional to the measured ambient field, and, with some additional processing, is the output of the sensor. The device is referred to as a "Fluxgate" due to the flux "gating" effect in the saturation state.

In practice, single rod core fluxgate sensors are quite impractical due to presence of a significant excitation signal in the sense voltage. Twin rod cores sharing one pick up coil or a configuration using a ring shaped core can be employed to mitigate this issue [32, 40, 23]. As an example of a device using two parallel rod cores is the Vacquier fluxgate sensor as presented in Fig. 2.5.

This sensor topology consists of two parallel rod cores, two excitation windings and one common pick up coil. The excitation windings are wound in opposite directions which causes the magnetic field driving the coils to saturation to be in opposite directions as well. In the absence of an ambient magnetic field the two cores reach saturation simultaneously, therefore no voltage is induced in pick up coil due to zero net flux. In a presence of an external magnetic field, a difference between the two coils is observed, which induces the sense voltage  $V_s$  in the pick up coil.

The ring core fluxgate sensor operates similarly to the Vacquier sensor. The ring core can be considered as two half-cores with excitation windings wound in opposite directions.

Similarly to Hall Effect Sensors, Fluxgate devices can be designed in Open and Closed Loop configurations. This type of magnetic sensor demonstrates excellent sensitivity and temperature stability, the ability to measure both AC and DC, low power dissipation, and galvanic isolation between the primary conductor and the output circuit. However, Fluxgate sensors are popular only within high accuracy applications due to their high cost [43, 33, 28].

### 2.3.6 Magneto Resistance Effect Sensors

Magneto Resistance Effect Sensors exploit the property of certain materials to vary their resistance as a function of external magnetic field. This analysis is focused on the most popular sensor designs based on Anisotropic Magneto Resistance (AMR), Giant Magneto Resistance (GMR) and Tunneling Magneto Resistance (TMR).

#### 2.3.6.1 Anisotropic Magneto Resistance Sensors

In some ferromagnetic materials such as Permalloy, a dependency of their electrical resistance on the applied magnetic field can be observed. If a current is induced through a thin film Permalloy strip, the material resistance is a function of the angle between the direction of current flow and the magnetization of the material. In a presence of an ambient magnetic field, this magnetization changes the direction toward the direction of the external field, and the angle of rotation is determined by the magnitude of the applied field.

If a current  $I$  flows along the x-axis of a Permalloy strip, the material magnetization direction corresponds to the direction of the current. Consequently, the angle  $\Theta$  between these two vectors is equal to 0, and the initial resistance is  $R_0$ . The strip resistance under the influence of an ambient magnetic field can be described as :

$$R(\Theta) = R_0 - \Delta R \sin^2(\Theta), \quad (2.4)$$

It can be clearly observed from the equation 2.4 that single-strip AMR sensor doesn't provide any information about the direction of the ambient field. A technique

called "barberpole biasing" is normally applied to account for this. Aluminum bars are deposited into the Permalloy strip at 45 degree angle as is illustrated in Fig. 2.6.

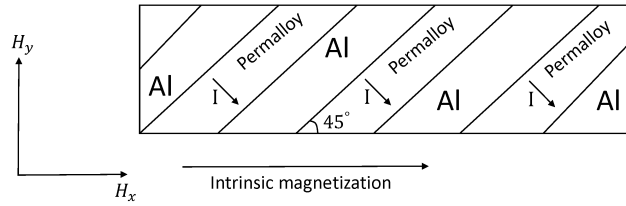


**Figure 2.6:** An AMR sensor with barber poles.

Due to aluminum's resistance being five times lower than that of Permalloy the direction of the current is driven to be at a 45 degree angle to the intrinsic magnetization. Therefore, it becomes possible to determine the applied field polarity [24, 25, 26, 22, 39].

AMR sensors experience high non-linearity and high temperature drift. Besides that, they are sensitive to parasitic magnetic fields that can affect the initial magnetization direction. In order to combat these issues, commercially available AMR current sensors employ a Wheatstone bridge configuration and additional compensation techniques (Fig. 2.7).

This sensor design utilizes a differential magnetic field measurement approach. Four barberpole magneto resistors are connected in a Wheatstone bridge configuration. The primary current  $I_p$  flows through a U shape conductor placed underneath of the bridge resistors. A compensation current  $I_{comp}$  is fed through a compensation conductor. The output voltage signal is then measured across resistor  $R_s$  [43, 22, 10].

F.W.Bell and Sensitec manufacturers supply products with  $\pm 0.8\%$  accuracy and current range up to 150A [10, 5].

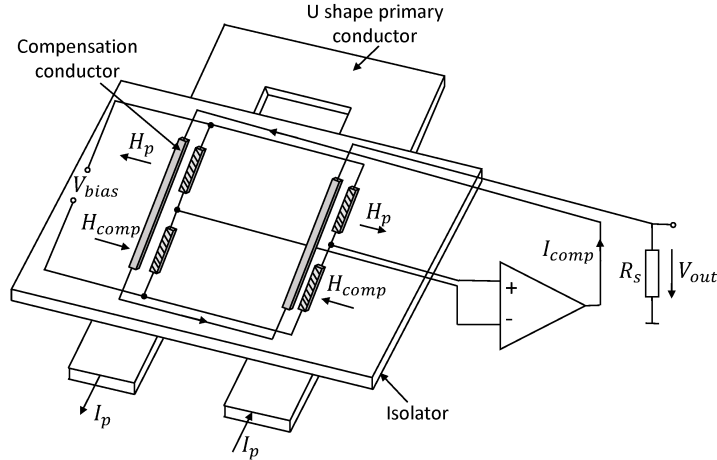


**Figure 2.7:** F.W Bell AMR current sensor.

### 2.3.6.2 Giant Magneto Resistance Sensors

Resistance changes in the presence of an external magnetic field has also been observed in a stack of thin magnetic and non-magnetic materials layers. Because this differential resistance is significantly larger (up to 15%) relative to the resistance change of anisotropic materials( 2%-4%), it is called "giant magnetoresistance".

The basic GMR element structure is comprised of two ferromagnetic layers (Fe, Co, Ni or their alloys) separated by a non-magnetic conductor (Cr, Cu, Ag, Au). If the current is fed through the GMR stack in the absence of an external magnetic field, the stack exhibits high resistance due to antiparallel magnetic moments in the ferromagnetic layers. In the presence of an externally applied magnetic field, the resistance decreases due to the magnetization of the magnetic layers being aligned in parallel. This type of sensor is only suitable for high magnetic field sensing due to imminence of anti-ferromagnetic coupling overcoming [43, 30, 35, 36].

An alternative GMR structure called the "Spin-valve" extends the sensor sensitivity range (Fig. 2.8). This allows this type of GMR structure to detect currents below the ranges of Hall-Effect or AMR sensors.

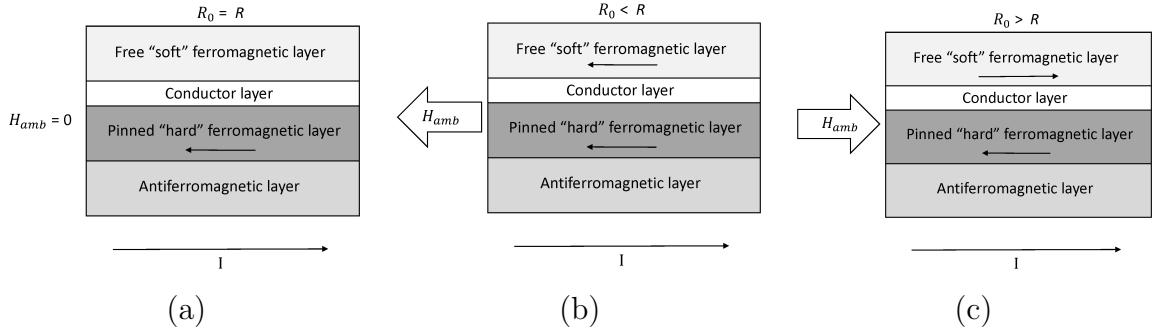


**Figure 2.8:** Spin-valve GMR sensor: (a) No external magnetic field. (b) External magnetic field parallel to pinned ferromagnetic layer. (c) External magnetic field antiparallel to pinned ferromagnetic layer.

The Spin-valve is a four layer structure with a conductor sandwiched between two ferromagnetic layers. One of the layer's magnetic moments is pinned by an antiferromagnetic layer, and is referred to as a "hard" ferromagnet. The free ferromagnetic layer is then called "soft". The magnetization of the free layers is dictated by the external magnetic field. This is due to the difference in spin-dependent electron scattering between the parallel and antiparallel magnetization orientations in hard and soft layers. The apparent resistance then decreases and increases respectively.

Unfortunately, GMR sensors exhibit high thermal drift and non-linearity. Similarly to AMR devices, GMR elements are often connected in a Wheatstone bridge configuration to improve these characteristics. The most common use of GMR sensors is in low power consumption, low current sensing. Allegro MicroSystems LLC supplies high sensitivity IC GMR current sensors with up to 5A current range [43, 23, 24, 31, 7].

### 2.3.6.3 Tunneling Magneto Resistance Sensors

TMR sensors employ the magnetic tunnel junction (MTJ) effect, which produces a much greater variation in resistance relative to GMR sensors ( up to 200% of greater resistance change at room temperature). The stuck structure is similar to the spin-valve GMR element, but the conducting layer is replaced with an insulator (typically  $MgO$  or  $Al_2O_3$ ). If an external magnetic field is applied, the magnetization direction

of the pinned and free layers can vary from parallel to antiparallel alignment. When the magnetic moments are parallel, electrons can tunnel through the insulation layer. The MTJ element experiences low resistance increasing with magnetic moments orientation aiming to antiparallel alignment.

In comparison with Hall-Effect, AMR, and GMR sensors, TMR technology provides wider sensitivity range, better linearity and thermal stability as well as low power consumption. However, TMR sensors have only recently been employed as current sensors commercially, and only by a few vendors ( MultiDimension Technology Co.,CotoTechnology) [24, 36, 4].

## 2.4 Possible solutions

The goal of this section is to narrow the list of commercially available current sensors analyzed in the previous section to the most potentially successful candidates for future consideration. A comparison of current sensing techniques according to the most important system requirements from Table 2.1 is listed in Table 2.2<sup>1</sup>.

**Table 2.2:** Comparison of potential current sensors for EVSE application.

Sensor type	AC/DC	Accuracy $\leq 0.5\%$	AC $\geq 120A$	Thermal stability	Approximate cost, \$
Shunt	yes	yes	yes	good	12
Rogowski coil	no	no	yes	very good	12
CT	no	yes	yes	good	14
Open-Loop Hall Effect	yes	no	yes	poor	22
Closed-Loop Hall Effect	yes	no	yes	good	32
Fluxgate	yes	yes	yes	very good	8.11 <sup>2</sup> and 150 <sup>3</sup>
AMR	yes	no	yes	fair	50
GMR	yes	yes	no	fair	6
TMR	yes	yes	yes	good	2

<sup>1</sup> Approximate cost data from Digi-Key Electronics, Mouser Electronics, EKM Metering, GMW Associates, F. W. Bell, NVE Corporation, ALLIED Electronic Automation, Coto Technology.

<sup>2</sup> The price for a product that requires extra design steps to meet the listed accuracy.

<sup>3</sup> The price for ready-to-use product.

After reviewing the sensor characteristics presented in Table 2.2, it is clear that Rogowski coils and CTs should be excluded from the list due to their inability to measure DC current. It is also apparent that Open-Loop Hall Effect and AMR sensors don't satisfy the accuracy and thermal stability requirements, and that GMR sensors are not suitable for high current applications. Consequently they should be also removed from the potential candidates list. Finally, Closed-Loop Hall Effect sensors should be excluded from the list of good candidates since the product meeting 0.5% accuracy of reading over the full range of 120 A, to the best of our knowledge, is not available on the market. Therefore, the final set of current sensing technologies will contain following sensor types:

- Shunt
- Fluxgate sensors
- TMR sensors

Future research should include detailed analyses focused on these current sensing techniques with respect to the V2G EVSE DC injection monitoring application.

## 2.5 Conclusions

Prevention of DC injection is a critical issue for power electronics, especially in the context of EV charging and V2G technology. Widespread adoption of power to grid will require adherence to power quality standards.

We proposed that the EVSE should have a high-precision cost-effective current sensing system with AC measurement and DC injection detection capabilities to provide extra safety to the grid if verified on-board power converter fails.

We carried out the review of various current sensing techniques potentially suitable for this application, and selected the most promising candidates for future research work.

## **2.6 Acknowledgement**

The work presented in this paper was funded by a grant from Nuvve Corp. to the University of Delaware. The authors thank Garrett Ejzak from University of Delaware for valuable advice and comments.

## REFERENCES

- [1] Iec 62053-11:2003, electricity metering equipment (a.c.) - particular requirements - part 11: Electromechanical meters for active energy (classes 0.5, 1 and 2). International standard, International Electrotechnical Commission, 2003.
- [2] Hall-effect open-loop current sensor application. Technical report, Honeywell, February 2007.
- [3] American national standard for electricity meters 0.1, 0.2 and 0.5 accuracy classes. Approved american national standard, American National Standards Institute, Inc, 2017.
- [4] The evolution of magnetic sensing technology: From hall effect to tunneling magnetoresistance (tmr). Technical report, Coto Technology, 2017.
- [5] Cds4000 family: Compact amr current sensors with overcurrent detection. Technical report, Sensitec, 2018.
- [6] Ieee 1547-2018, ieee standard for interconnection and interoperability of distributed energy resources with associated electric power systems interfaces. Standard, IEEE, 2018.
- [7] Acs70331: High sensitivity, 1 mhz, gmr-based current sensor ic in space-saving low resistance qfn and soic packages. Technical report, Allegro microsystems, 2019.
- [8] Specifications, tolerances, and other technical requirements for weighing and measuring devices. Standard, National Institute of Standards and Technology Handbook 44, 2020.

- [9] An introduction to the hall effect. Technical report, Bell Technologies Inc, n.d.
- [10] Magneto-resistive current sensors for peak currents up to 150a. Technical report, F.W. Bell, n.d.
- [11] Ahmed Abdelhakim, Paolo Mattavelli, Dongsheng Yang, and Frede Blaabjerg. Coupled-inductor-based dc current measurement technique for transformerless grid-tied inverters. *IEEE Transactions on Power Electronics*, 33(1):18–23, 2018. doi:10.1109/TPEL.2017.2712197.
- [12] Farag Berba, David Atkinson, and Matthew Armstrong. A new approach of prevention of dc current component in transformerless grid-connected pv inverter application. In *Power Electronics for Distributed Generation Systems (PEDG), 2014 IEEE 5th International Symposium on*, pages 1–7. IEEE, 2014. doi:10.1109/PEDG.2014.6878638.
- [13] Juan Manuel Carrasco, Leopoldo Garcia Franquelo, Jan T. Bialasiewicz, Eduardo Galvan, Portillo Guisado, Ramon C., Martin Prats Ma. Angeles, Jose Ignacio Leon, and Narciso Moreno-Alfonso. Power- electronic systems for the grid integration of renewable energy sources: A survey. *IEEE Transactions on Industrial Electronics*, 53(4), August 2006. doi:10.1109/TIE.2006.878356.
- [14] Loredana Cristaldi, Alessandro Ferrero, Massimo Lazzaroni, and RT Ottoni. A linearization method for commercial hall-effect current transducers. *IEEE transactions on Instrumentation and Measurement*, 50(5):1149–1153, 2001. doi:10.1109/19.963175.
- [15] Bill Drafts. Understanding hall effect devices. *Sensors-the Journal of Applied Sensing Technology*, 14(9):72–74, 1997.
- [16] Luka Ferkovic, Damir Ilic, and Roman Malaric. Mutual inductance of a precise rogowski coil in dependence of the position of primary conductor.

- IEEE transactions on instrumentation and measurement*, 58(1):122–128, 2009. doi:10.1109/TIM.2008.928412.
- [17] Javier García-Martín, Jaime Gomez-Gil, and Ernesto. Vázquez-Sánchez. Non-destructive techniques based on eddy current testing. *Sensors*, 2011. doi:10.3390/s110302525.
- [18] Lars Gertmar, Per Karlsson, and Olof Samuelsson. On dc injection to ac grids from distributed generation. In *Power Electronics and Applications, 2005 European Conference on*, pages 10–pp. IEEE, 2005. doi:10.1109/EPE.2005.219420.
- [19] Willett Kempton and Jasna Tomić. Vehicle-to-grid power fundamentals: Calculating capacity and net revenue. *Journal of power sources*, 144(1):268–279, 2005. doi:10.1016/j.jpowsour.2004.12.025.
- [20] William Koon. Current sensing for energy metering. In *Conference Proceedings IIC-China/ESC-China*, pages 321–324, 2002.
- [21] Bill Kramer, Sudipta Chakraborty, and Benjamin Kroposki. A review of plug-in vehicles and vehicle-to-grid capability. In *Industrial Electronics, 2008. IECON 2008. 34th Annual Conference of IEEE*, pages 2278–2283. IEEE, 2008. doi:10.1109/IECON.2008.4758312.
- [22] Gerold Laimer and Johann W Kolar. Design and experimental analysis of a dc to 1 mhz closed loop magnetoresistive current sensor. In *Applied Power Electronics Conference and Exposition, 2005. APEC 2005. Twentieth Annual IEEE*, volume 2, pages 1288–1292. IEEE, 2005. doi:10.1109/APEC.2005.1453172.
- [23] Francis Laurent A. and Krzysztof Iniewski. *Novel Advances in Microsystems Technologies and Their Applications*. CRC Press, TaylorFrancis Group, 2016.
- [24] James Lenz and S Edelstein. Magnetic sensors and their applications. *IEEE Sensors journal*, 6(3):631–649, 2006. doi:10.1109/JSEN.2006.874493.

- [25] James E Lenz. A review of magnetic sensors. *Proceedings of the IEEE*, 78(6):973–989, 1990. doi:10.1109/5.56910.
- [26] Howard Mason. Basic introduction to the use of magnetoresistive sensors. Technical report, App Note 37, Zetex Semiconductors.(Last visited: 7 th November 2007), 2003.
- [27] Louie J Powell. Current transformer burden and saturation. *IEEE Transactions on Industry Applications*, (3):294–303, 1979. doi:10.1109/TIA.1979.4503656.
- [28] Fritz Primdahl. The fluxgate magnetometer. *Journal of Physics E: Scientific Instruments*, 12(4):241, 1979. doi:10.1088/0022-3735/12/4/001.
- [29] John D Ramboz. Machinable rogowski coil, design, and calibration. *IEEE Transactions on Instrumentation and measurement*, 45(2):511–515, 1996. doi:10.1109/19.492777.
- [30] Candid Reig, Susana Cardoso, and Subhas Chandra Mukhopadhyay. Giant magnetoresistance (gmr) sensors. *SSMI6*, 1:3–5, 2013.
- [31] Damhuji Rifai, Ahmed Abdalla, Kharudin Ali, and Ramdan Razali. Giant magnetoresistance sensors: a review on structures and non-destructive eddy current testing applications. *Sensors*, 16(3):298, 2016. doi:10.3390/s16030298.
- [32] Pavel Ripka. Review of fluxgate sensors. *Sensors and Actuators A: Physical*, 33(3):129–141, 1992. doi:10.1016/0924-4247(92)80159-Z.
- [33] Pavel Ripka. Advances in fluxgate sensors. *Sensors and Actuators A: Physical*, 106(1-3):8–14, 2003. doi:10.1016/S0924-4247(03)00094-3.
- [34] Pavel Ripka. Current sensors using magnetic materials. *Journal of optoelectronics and advanced materials*, 6:587–592, 2004.

- [35] Ravinder Pal Singh and Ashwin M Khambadkone. Giant magneto resistive (gmr) effect based current sensing technique for low voltage/high current voltage regulator modules. *IEEE Transactions on Power Electronics*, 23(2):915–925, 2008. doi:10.1109/TPEL.2007.915771.
- [36] Enrique García Vidal, Diego Ramírez Muñoz, Sergio Iván Ravelo Arias, Jaime Sánchez Moreno, Susana Cardoso, Ricardo Ferreira, and Paulo Freitas. Electronic energy meter based on a tunnel magnetoresistive effect (tmr) current sensor. *Materials*, 10(10):1134, 2017. doi:10.3390/ma10101134.
- [37] Wei Wang, Ping Wang, Taizhou Bei, and Mengmeng Cai. Dc injection control for grid-connected single-phase inverters based on virtual capacitor. *Journal of Power Electronics*, 15(5):1338–1347, 2015. doi:10.6113/JPE.2015.15.5.133.
- [38] Chucheng Xiao, Lingyin Zhao, Tadashi Asada, WG Odendaal, and JD Van Wyk. An overview of integratable current sensor technologies. In *Industry Applications Conference, 2003. 38th IAS Annual Meeting. Conference Record of the*, volume 2, pages 1251–1258. IEEE, 2003. doi:10.1109/IAS.2003.1257710.
- [39] Liu Xuyang, K Lam, Ke Zhu, Chao Zheng, Xu Li, Yimeng Du, Liu Chunhua, and Philip Pong. Overview of spintronic sensors with internet of things for smart living. *IEEE Transactions on Magnetics*, PP, 07 2019. doi:10.1109/TMAG.2019.2927457.
- [40] Xiaoguang Yang, Yuanyuan Li, Weidong Zheng, Wei Guo, Youhua Wang, and Rongge Yan. Design and realization of a novel compact flux-gate current sensor. *IEEE Transactions on Magnetics*, 51(3):1–4, 2015. doi:10.1109/TMAG.2014.2358671.
- [41] Murat Yilmaz and Philip T Krein. Review of battery charger topologies, charging power levels, and infrastructure for plug-in electric and hybrid vehicles. *IEEE Transactions on Power Electronics*, 28(5):2151–2169, 2013. doi:10.1109/TPEL.2012.2212917.

- [42] Weichi Zhang, Matthew Armstrong, and Mohammed Elgendy. Dc current determination in grid-connected transformerless inverter systems using a dc link sensing technique. In *Energy Conversion Congress and Exposition (ECCE), 2017 IEEE*, pages 5775–5782. IEEE, 2017. doi:10.1109/ECCE.2017.8096958.
- [43] Silvio Ziegler, Robert C Woodward, Herbert Ho-Ching Iu, and Lawrence J Borle. Current sensing techniques: A review. *IEEE Sensors Journal*, 9(4):354–376, 2009. doi:10.1109/JSEN.2009.2013914.
- [44] A. F. Zobaa and C. Cecati. A comprehensive review on distributed power generation. *International Symposium on Power Electronics, Electrical Drives, Automation and Motion. SPEEDAM*, 2006. doi:10.1109/SPEEDAM.2006.1649826.

## Chapter 3

### INTEGRATED ELECTRIC VEHICLE SHUNT CURRENT SENSING SYSTEM FOR CONCURRENT REVENUE METERING AND DETECTION OF DC INJECTION

*After reviewing eight current sensing technologies in Chapter 2, the shunt was selected from the list of suitable sensors as the simplest and inexpensive solution. Chapter 3 introduces the current sensing system we designed, prototyped and validated based on the integrated shunt. First, we introduce the problem's background and the sensing system design requirements. Next, we explain the operating principle of the shunt, its advantages and drawbacks as well as a motivation behind the sensor selection. Next, we list the design challenges and concerns such as the system power dissipation and energy losses due to the shunt. After that we introduce the prototype components as well as the design to integrate the prototype into a single and three phase EVSE. Further, we demonstrate the prototype's validation. The results include the accuracy of AC current measurements for charging and discharging, ability to detect DC injection of  $\geq 400$  mA in a presence of AC currents up to 80 A, and DC injection detection accuracy at the limit value. Finally, we demonstrate the cost-effectiveness of the designed system over today's common practice of a the current transducer (CT).*

#### **3.1 Abstract**

Even certified electric vehicle power converters can inject DC into AC grid if they fail. Due to significant scrutiny of Vehicle-to-Grid technology from regulators, detection of DC injection is especially important during bidirectional electric vehicle charging. Verification of DC injection by the Electric Vehicle Supply Equipment, can be a cost-effective extra measure to ensure power quality from a variety of plugged-in

electric vehicles. As the Electric Vehicle Supply Equipment also performs high accuracy revenue energy metering, measurement of AC current and DC injection with a single sensor is the most economically efficient way. This paper presents an Integrated Shunt current sensing system for inexpensive concurrent revenue metering and DC injection detection by 19.2kW single-phase Electric Vehicle Supply Equipment, and outlines how it would be extended to 100kW three-phase Electric Vehicle Supply Equipment. The prototype can detect DC injection of  $\geq 400$  mA in AC current up to 80 A in accordance with the IEEE 1547-2018 standard. The prototype can also conduct revenue metering within 1.0 accuracy class. The prototype doesn't demonstrate essential power dissipation at high currents typical for shunt systems. Finally, the prototype is cost-competitive with common Electric Vehicle Supply Equipment revenue metering system which cannot detect DC injection.

### 3.2 Introduction

Today's power generation systems include a variety of distributed energy resources (DERs), which are capable of supplying AC to the grid when it is demanded [17]. All DERs, connected to the grid, must ensure the power quality by limiting the DC injection to less than 0.5% of the full rated output current, according to the "Limitation of DC injection" IEEE 1547-2018 standard [4]. DC injection is when a small portion of DC current is superimposed on an AC current during power conversion. Significant amounts of DC injection affects the power quality by causing a variety of negative effects on other grid equipment [12, 23].

Electric Vehicle's (EV's) batteries can be used as short-term storage for excess energy generated by renewable sources such as wind and solar. This energy can then be injected back to the grid during peak hours for rapid response to electricity demand. This technology, developed at the University of Delaware, is called Vehicle-to-Grid (V2G) [13].

An important part of a V2G system is the Electric Vehicle Supply Equipment (EVSE). A V2G aware EVSE is capable of controlling single or three-phase power flow

between a vehicle and the grid in accordance with an appropriate control signal [16]. Because of the possibility of power injection back to the grid, we propose that EVSEs must verify the DC injection level from whatever EV might be connected. Verification of DC injection by the EVSE can be a cost-effective extra safety measure, as DC can be injected even from verified EV's power converter if it fails. DC injection is also possible with a unidirectional (charge only) power converter in the EV, but even if only because regulators are more wary of bidirectional charging we consider it especially important to detect DC injection in this case.

In addition to DC injection detection, EVSEs must conduct high accuracy AC current measurements to meet revenue metering requirements of various regional transmission operators (RTOs) [18, 1]. The least expensive implementation of concurrent revenue metering and DC injection detection is to employ the single sensor for both types of measurements.

As shown in previous research [16], there are several existing methods of DC injection mitigation that can be implemented by the power electronics of a power converter [9, 21, 8]. However, none of them are suitable for EVSE as they are a gateway through which different EVs plug in, with their own power converters. Preventive methods are implemented by the inverter and integrated into the inverter's circuitry. An EVSE must sense, not prevent DC injection since it is a separate device, protecting the building equipment and grid from a variety of EVs. As a result, EVSE application requires a new solution compatible with different types of power converters.

The paper presents the design, prototype and validation of an Integrated Shunt current sensing system with concurrent revenue metering and DC injection detection capabilities for 19.2kW single phase EVSEs with perspective extension to 100kW three phase EVSEs. As a result, the system can be a cost-effective way to connect EV's equipment and the grid, preventing faulty injection current going into AC grid by detecting the dangerous level of DC injection and interrupting the connection.

### 3.3 Prototype Design

#### 3.3.1 System Requirements

The current sensing system requirements for bidirectional EVSEs are listed in Table 3.1.

**Table 3.1:** The current sensing system requirements for bidirectional EVSEs.

Parameters	Requirements	
	Single phase unit (19.2 kW)	Three phase unit (100 kW)
Voltage (L-N)	120V, 230V	120V, 230V, 277V, 347V
DC injection limit	0.5% of $I_{rated}$	
DC injection detection accuracy at the limit value	10-20%	
AC current metering accuracy classes	0.5, 1.0, 2.0	
$I_{rated}$	80A	120A
Cost	Low	

First, the system must be suitable as much as possible for global utility voltages. Second, after detecting DC injection, the sensing system should disable charging/discharging, if the DC injection level exceeds 400 mA for single-phase units and 600 mA for three-phase units with respect to the "Limitation of DC injection" section in IEEE 1547-2018 standard (see 3.2). As DC injection detection accuracy requirements are not specified in the standard, authors estimated accuracy of 10%-20% to be sufficient for proper detection of DC injection.

In addition to DC injection detection, the sensing system should allow for AC current measurements up to  $I_{rated}$  with required accuracy (see 3.2). The EVSE metering accuracy classes, listed in a Table 3.1, are measured at a low and a high current of the EVSE under test (TESCO Engineering test report "EV Meter Accuracy Testing")

for University of Delaware) [5]. Low current is defined as 10% of the rated current. High current is defined as 85% of the rated current according to NIST Handbook 44 (HB-44), Section 3.40 "Electric Vehicle Fueling Systems" [7]. Accuracy classes criteria are defined from NIST HB-44 with reference to ANSI C.12-20 standard [7, 2].

Ideally, the sensing system should meet all three accuracy classes to fulfil the revenue metering requirements of a great variety of RTOs. At the same time, the system performance within 1.0 or 2.0 accuracy classes will be sufficient for certain RTOs, such as PJM[3].

Finally, authors are aiming for low total system's cost to facilitate mass production of EVSEs.

### 3.3.2 Selecting the Current Sensor

The most economical way to implement the system is to measure AC current along with DC injection with a single device. Currently, AC current in University of Delaware's EVSEs is measured by the most common EVSE current sensor: the current transformer (CT). Unfortunately, due to its incapability of DC current detection, CT cannot serve both purposes [16].

A great variety of current sensors are presented on the market and as research prototypes. Although they demonstrate outstanding performance results, not all of the sensors are able to meet all the EVSE system requirements (see Table 3.1). For instance, the Hall Effect on-chip sensor, presented in [10], and magnetoresistive sensor, presented in [15], show promising performance results. However, they have limited operating current range much below the range required for application in question. Although, the authors assert that the current range can be extended in the future, no results are currently presented. In addition, Ref. [16] demonstrates that commercially available current sensors such as Rogowski coils, Hall-Effect sensors, anisotropic magnetoresistance (AMR) sensors and giant magnetoresistance (GMR) sensors are not suitable for the application in question. For instance, Rogowski coil is not capable to detect DC current, GMR sensor has limited operating current range, and Hall-Effect

and AMR sensors lack standards-required AC accuracy at small currents. Ref. [16] also demonstrates that shunt, fluxgate and tunneling magnetoresistance (TMR) current sensors are the most promising candidates as they are able to meet all the system's requirements. Considering the cost of fluxgate, and complexity and limited availability of TMR sensors, shunt was selected from the list of suitable sensors as the simplest and inexpensive solution.

### **3.3.3 Shunt current sensor operating principle**

A shunt is one of the simplest current sensing techniques capable of measuring both AC and DC current. The fundamental operating principle of the shunt is Ohm's Law of Resistance. The measured voltage drop across the shunt is proportional to the current flowing through the sensor [20].

In addition to AC and DC measurement capability and simplicity, shunts are a low cost current sensing solution with an acceptable level of accuracy. Typical accuracy numbers for a shunt are  $\pm 0.1\%$ ,  $\pm 0.25\%$ ,  $\pm 0.5\%$ . Such high precision shunts are made possible by making them out of low thermal drift alloys which can have a thermal coefficient of resistance (TCR) of around  $<20$  ppm/ $^{\circ}\text{C}$  [14].

The potential drawbacks of shunt-based current sensors include: the absence of galvanic isolation, power dissipation in the shunt itself producing heat, and a need for signal amplification due to a voltage drop of only a few micro-volts [19, 22].

### **3.3.4 Design Challenges**

#### **3.3.4.1 Single Sensor for AC and DC Measurements**

As was discussed in 3.3.2, the solution should employ a single sensor for both AC and DC measurements. The challenge in this approach is that the AC signal to be measured is two orders of magnitude larger than the expected DC signal (see Table 3.1), and, therefore, it is complicated to measure them effectively simultaneously.

### 3.3.4.2 High-Side Current Sensing

Due to the structure of US residential utility system and the EVSE, the only way to measure current with a shunt is high side current sensing. This implies the presence of extremely high input common-mode voltage (Table 3.1) relative to the signal of interest, which makes it impossible to measure the AC current with the required precision with the typical high side current sensing approach of an amplifier designed for this purpose. This is due to the presence of parasitic common-mode voltage at the output of the difference amplifier, which is significantly greater than the allowable error of AC current measurements. Based on the required AC current metering accuracy, the minimum AC current to be measured (3.3.1) and the shunt resistance  $R = 280 \mu\Omega$ , the allowable voltage error is  $V_{error} = 11.2 \mu\text{V} \pm 5\%$  due to the shunt tolerance. Ten AD8479 unity gain difference amplifier's output voltages were measured in presence of 120 A common-mode voltage with no current flowing through the shunt. Test results show the parasitic voltage to be  $V_p = 3.36 \text{ mV}-12 \text{ mV}$  depending on the common-mode rejection ratio (CMRR) of the particular amplifier being tested (Table 3.2). These results are in-line with the theoretical calculations below:

$$V_p = A_d(V_+ - V_-) + \frac{1}{2}A_{cm}(V_+ + V_-) \quad (3.1)$$

where  $A_d = 1$  and  $V_+ = V_- = 120 \text{ V}$  at  $I = 0 \text{ A}$ .

Common-mode voltage gain  $A_{cm}$  can be obtained from the equation:

$$CMRR = 20 \log_{10}\left(\frac{A_d}{A_{cm}}\right)dB \quad (3.2)$$

where  $CMRR = 80-90 \text{ dB}$ .

After calculating  $A_{cm}$ , we can obtain the value of  $V_p$  from equation 3.1, so that  $V_p = 3.8 \text{ mV}-12 \text{ mV}$ . The measured minimum  $V_p$  is lower than calculated value. The difference can possibly be a result of exceptional performance of one particular amplifier with CMRR above data sheet specification. Alternatively, it could be a result

of a measurement error due to a difficulty to measure very low signals accurately. Nevertheless, the difference does not affect the overall conclusion.

### 3.3.4.3 Power Dissipation and Energy Losses

Due to the shunt being installed into the conductive path, power dissipation and associated energy losses occur. This needs to be considered in the design.

### 3.3.5 Power and Energy Losses due to the Shunt

As mentioned in 3.3.4.3, the shunt power dissipation must be considered as a potential problem due to excessive heat generation and energy/financial losses. In order to estimate the problem, following calculations are considered:

$$P_{loss} = I^2 R \quad (3.3)$$

where  $P_{loss}$  is continuous power loss across the shunt,  $I = 60$  A (typical operation),  $R = 280 \mu\Omega$ . Assuming an EV is performing a regulation service (20% duty cycle,  $t_{reg} = 22$  hours and  $t_{ch} = 1$  hour/day). Therefore energy loss  $E_{loss}$  can be calculated:

$$E_{loss} = P_{loss}(t_{ch} + t_{reg} \cdot 0.2) = 5.94 \text{ Wh/day} \quad (3.4)$$

or  $\sim 2$  kWh/year.

Typical energy cost in the US is approximately 12 cents/kWh [6]. Consequently the losses due to the shunt would be approximately  $\sim 30$  cents/year, this is inconsequential relative to the cost-savings over the incumbent solution (approx. \$3 compared to \$14 for the BCT-013-200 CT) [11].

### 3.3.6 Prototype System Components

The single phase system block diagram is presented on figure 3.1

The current monitoring system is integrated into the EVSE hardware and consists of two major blocks: the current sensor hardware block and the micro controller signal processing block.

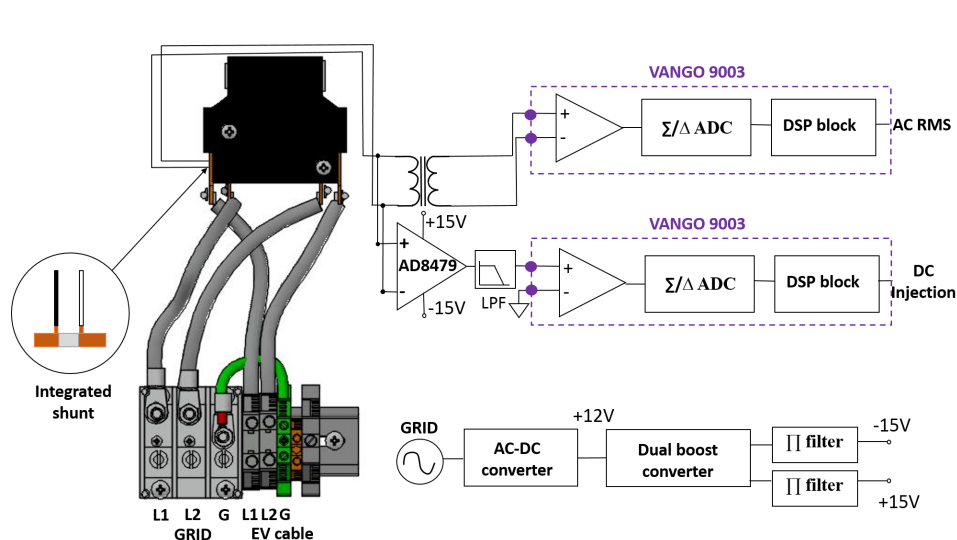


**Figure 3.1:** Current sensing single phase system block diagram.

The sensor part is comprised of a shunt resistor integrated into a latching relay manufactured by KG Technology, Inc. The relay’s primary function is to de-energize the EV’s connection point when a vehicle is not actively charging or providing grid services. It is also used as the disconnection element in the EVSE’s integrated residual current device (RCD) (also known in North America as a ground-fault circuit interrupter (GFCI)). It can also be used to disconnect the circuit in the event of a DC injection fault if the vehicle fails to comply with a request to stop charging/discharging.

There are two readout circuits for the single shunt sensor. In the first, the AC component is extracted via a signal isolation transformer (TTC-5036). This signal is passed directly to the one of the current inputs of a Vango 9003 metrology chip. This chip was designed primarily for use in smart energy meters.

In the second circuit the shunt signal is captured by a unity gain difference amplifier (AD8479). This amplifier is designed for high-voltage high-side sensing applications and, therefore, has a high input common mode voltage range and a high CMRR. The AD8479 requires a  $\pm 15$  VDC power supply. In the proposed design this

dual 15 VDC power supply is provided by a boost power converter (LT1945EMS) powered by the same AC-DC LPF-16-12 power supply that powers the rest of the EVSE.

Although the DC injection detection circuit fails to block all of the AC common-mode signal, only the DC component is of interest. The Vango 9003 is capable of isolating AC and DC components of its analog inputs and, therefore, the parasitic common-mode voltage at the output of the amplifier doesn't impact the measurements. A first-order RC low pass filter with cut-off frequency of 1 Hz is included to decrease the AC signal component to prevent saturation of the 9003's inputs if the particular amplifier has relatively low CMRR. The filter has a gain of -17.5 dB at 60 Hz frequency.

The signal is then processed by the Vango 9003 metrology chip. As mentioned above, the signal is split into AC and DC components by a decimation filter. As a result, the DC injection value can be detected and compared with the threshold for further actions like error message generation, requests for the vehicle to stop charging, and/or opening the relay. Vango 9003 updates AC and DC measurements once per 20ms and stabilizes in 80ms.

All the elements are intended to be integrated into a printed circuit board (PCB) which also provides residual current detection and activates the safety relay. However, due to the timing and cost of the board fabrication constrains, the proof-of-concept prototype presented in this paper is designed on a separate small PCB board attached to the main one in several connection points.

This single-phase design can be extended to three-phases by installing shunt sensors and signal extraction circuitry for each of the three-phases. The Vango 9003 is capable of single and three-phase metering so there is no need to change the metering chip or to add more of them. <sup>1</sup>

---

<sup>1</sup> Fig. 1 shows utilization of two separate Vango 9003 microcontrollers for AC measurements and DC detection. We believe, however, that only one 9003 is required if DC detection is performed with the microcontroller's auxiliary analog input with each phase being measured in turn. This solution will reduce the total cost of the system, which is critical for mass production of EVSEs.

Specifications for the primary components of both the single and three phase systems can be found in Table 3.2.

**Table 3.2:** Main design parts specification.

Part name	Part number	Specifications
Relay with shunt integrated (single phase)	K237X-S006P -2AT-C946	Max current rating: 100 A Shunt resistance: $280 \mu\Omega$ Shunt tolerance: $\pm 5\%$ Shunt Temperature Coefficient of Resistance (TCR): $15 \text{ ppm}/\text{C}^\circ$
Relay with shunt integrated (three phase)	K316X-S006P -3BT-C1047	Max current rating: 120 A Shunt resistance: $280 \mu\Omega$ Shunt tolerance: $\pm 5\%$ Shunt Temperature Coefficient of Resistance (TCR): $15 \text{ ppm}/\text{C}^\circ$
Signal transformer	TTC-5036	Frequency range: 200 Hz-4 kHz Voltage isolation: $1875 V_{rms}$ @1 s
Difference amplifier	AD8479	$V_{CM} = 600 \text{ V}$ $V_s = \pm 15 \text{ V}$ CMRR = 80 dB-90 dB Gain = 1
Signal processing microcontroller	Vango9003	Three-phase multi-functional energy meter

### 3.4 Prototype Validation

We tested the prototype against three major requirements: the accuracy of bidirectional (EV charging/discharging) AC current measurement, the DC injection detection accuracy at the limit value of 400 mA, and potential effect of a large AC current on DC injection detection.

#### 3.4.1 Accuracy of AC current measurements

Table 3.3 shows bidirectional AC current measurements from the Vango 9003 AC RMS channel using the prototype after the initial coarse hand calibration.

**Table 3.3:** AC current measurements for charging and discharging.

Charging					Discharging				
$I_{ref}$ (A)	$I_m$ (A)	$S(\overline{I_m})$ (A)	Bias error (%)	Precision error (%)	$I_{ref}$ (A)	$I_m$ (A)	$S(\overline{I_m})$ (A)	Bias (%)	Precision error (%)
6	6.15	0.055	2.5	0.89	6	5.93	0.052	1.1	0.87
10	10.14	0.052	1.38	0.52	10	9.96	0.052	0.38	0.52
15	15.09	0.041	0.57	0.37	15	15.95	0.055	0.33	0.37
20	20.09	0.041	0.43	0.20	20	19.99	0.041	0.07	0.20
35	35.2	0.000	0.57	0.00	35	35.06	0.052	0.18	0.15

The reference AC current  $I_{ref}$  was provided by a Calmet C300B three-phase power calibrator and tester with a rated accuracy of 0.05 %. Reference currents of 6 A, 10 A, 15 A, 20 A and 35 A were applied across the shunt in a presence of a common mode voltage  $V_{cm} = 120$  V (L-N single-phase). Mean value  $\overline{I_m}$ , standard deviation  $S(\overline{I_m})$ , bias error and precision error were calculated for each value of a reference current. Presumably assuming that bias error can be calibrated to near 0 value after careful fine calibration, the precision error is reported as an accuracy.

Note that only currents of maximum and minimum current test conditions were considered for the system’s accuracy class estimation (see 3.3.1). Other measurements are provided only for a reference. The measurements demonstrate that for charging and for discharging, the sensing system meets 0.5 accuracy class requirements for maximum current of 35 A, but the system does not meet the same class requirements for a minimum current of 6 A. Note that the sensor satisfies the requirements for 1.0 class accuracy for both test conditions.

For the current prototype iteration, the factor limiting the accuracy of the system is the 0.1 A resolution of AC measurements, since the current is measured directly. However, in a complete EVSE measurement system, it is the power that is measured. The power measurement resolution is equal 0.01 W, enabling more precise calibration and higher precision current measurements, potentially leading to further error reduction.

In addition, we believe, that when the prototype circuit is integrated into the

RCD board, it will improve errors resulting from the current prototype’s imperfect connections. Therefore, for further calibration and error reduction, the prototype circuit must be integrated into the main board (see 3.3.6).

### 3.4.2 DC Injection Detection

#### 3.4.2.1 Accuracy of DC injection detection

In order to determine DC injection detection accuracy for positive and for negative DC injection, a Keithley 2410 SourceMeter was used to supply high precision DC current (0.034% source accuracy) of -1 A to 1 A through the shunt sensor, and the Vango 9003 DC channel’s response was recorded.

These data are illustrated in Fig. 3.2, which on the y-axis shows supplied DC current and on the x-axis shows linear function of DC current as measured by the current measuring system.

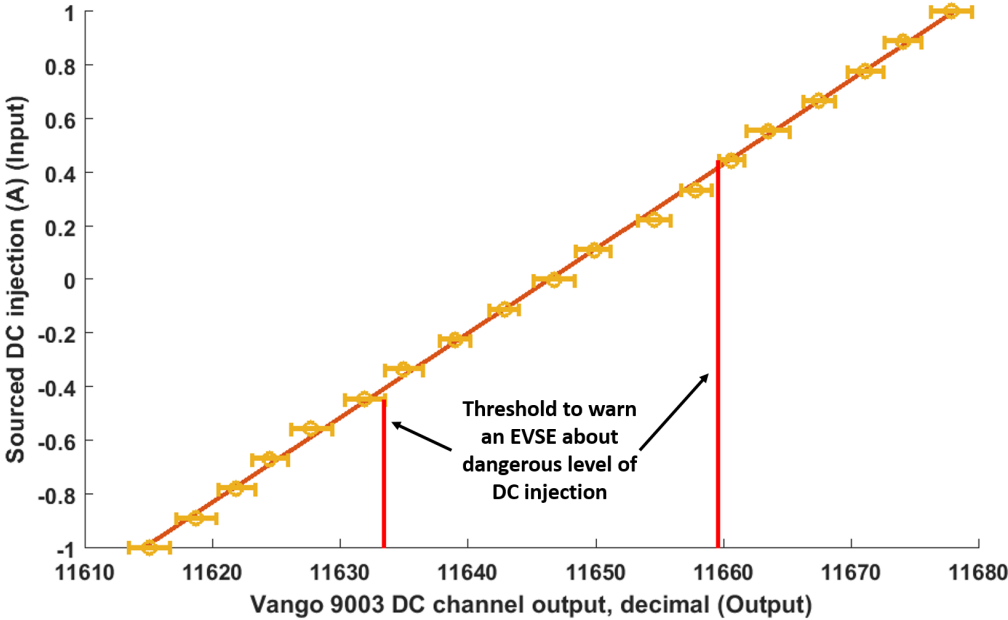


**Figure 3.2:** Setting the DC injection alarm threshold for positive (right line) and negative (left line) DC injection.

Each unit on x-axis represents 33 mA. The small horizontal lines show the mean and a standard deviation of each 20 measurements at 100 mA interval. DC injection alarm thresholds settings for charging and discharging are depicted by red vertical lines. These thresholds are set at one standard deviation ( $\sigma = 1$  or 33 mA (8.25% accuracy) for positive DC injection and  $\sigma = 2$  or 66 mA (16.5% accuracy) for negative DC injection) below 400 mA to ensure that in 84% cases the DC injection will not exceed the limit of 400 mA. Setting the threshold implies equivalent to the probability of a single measurement producing false negative is 16%. The adjustment of the thresholds that can be seen on the Fig. 3.2, is represented by shifting each red line toward 0 mA. Considering the alarm decision is planning to be made based on several data points in the complete system, the probability of false negatives decreases even further.

The non-linearity error is shown on Fig.3.3. The error doesn't exceed 4% of a full scale of 1A for both charging and discharging. We expect errors to be reduced further after the prototype is integrated into the RCD board.

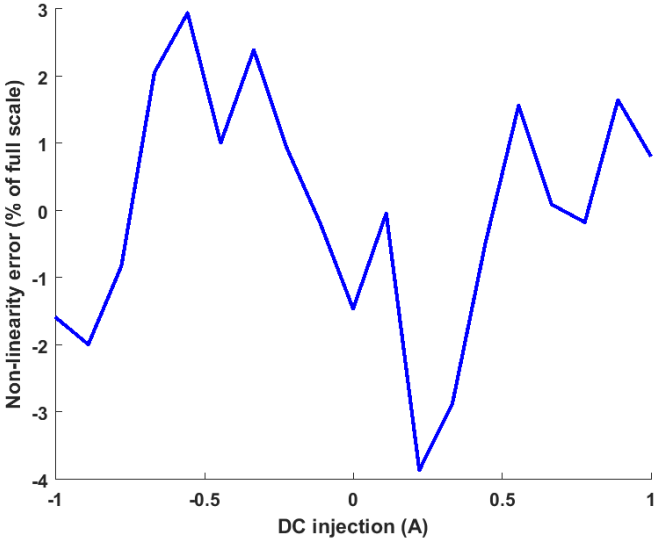


**Figure 3.3:** Non-linearity error (% of full scale).

### 3.4.2.2 Effect of large AC current on DC injection detection

Important factor potentially affecting the accuracy of DC injection detection is a presence of a large AC signal on the same line. In order to determine the effect of a large AC current on a DC injection reading, AC currents of 0.001 A and 80 A ( $I_{rated}$  for 19.2 kW single-phase EVSE) were applied across the shunt. The test current was provided by a Calmet C300B three-phase power calibrator and tester with a rated accuracy of 0.05 %. The output of DC injection channel was recorded at two AC current values. Assuming that each population is normally distributed, a two-sample  $t$ -test of two populations without assuming equal variances (Welch’s  $t$ -test) was applied. The  $t$ -test result confirms the null hypothesis at the 5% significance level. Therefore, we conclude that DC injection can be detected in a presence of a large AC currents without any significant distortion of the DC injection readings.

### 3.4.3 Prototype System Cost-Effectiveness

A comparison of the approximate cost of the system currently in use on single-phase EVSE units vs that of the prototype is provided in Table 3.4<sup>2</sup>.

**Table 3.4:** Systems cost comparison for single-phase EVSE.

CT+Hall Effect sensor			Shunt prototype system		
Part No	Qty	Price	Part No	Qty	Price
BCT-013-200 CT	1	\$14	Shunt	1	\$3
Vango 9003	1	\$3.15	Vango 9003	1	\$3.15
LEM LA-150P	1	\$19.04	AD8479ARZ-RL	1	\$4.25
			TTC-5036	1	\$2.52
			LT1945EMS	1	\$2.60
<b>Approximate total cost</b>		\$36.19	\$15.52		

For the system in use (the left section) prices are listed for the major components: CT BCT-013-200 and Vango 9003 metrology chip. Hall-Effect sensor LA-150P

<sup>2</sup> Price data compiled from Digi-Key Electronics, Mouser Electronics, Vango Technology, and KG Technologies for 1000+ quantity. Cost estimate doesn’t include parts with price below \$0.5.

with current range up to 150 A was added to cost comparison to represent an additional cost for DC injection detection.<sup>3</sup> For our prototype shunt system (the right section) prices are listed for a shunt, Vango 9003, difference amplifier AD8479ARZ-RL, isolation transformer TTC-5036 and a boost converter LT1945EMS. The prototype system's approximate total cost is less than half to that of the CT and Hall-Effect sensor.

### 3.5 Conclusions

A shunt-based AC and DC current sensing system for single-phase EVSEs has been designed, prototyped, and tested. This prototype has a potential to replace the BCT-013-200 CT based system currently in use in mass production EVSEs. The new system is independent of the type of inverter used in any EV and thus is capable of interconnection with all manner of EVs.

The prototype can simultaneously conduct high precision revenue metering and detect DC injection into the grid by EV's on-board equipment in case of a fault. This prototype is cost-effective relative to the system in use with added DC sensor.

Presumably assuming that the bias error of revenue metering current measurements will be decreased to near 0 value after fine calibration, the systems meets 1.0 accuracy class requirements for revenue metering.

The prototype can detect DC injection of 400 mA or more in an AC signals up to 80 A. DC injection detection resolution is 33 mA. Non-linearity error is below 4% of the full scale. The accuracy of positive DC injection detection at the limit value is 8.25% and 16.5% for negative DC injection. Due to extremely low shunt resistance, the prototype doesn't exhibit significant power losses at high currents, expected from shunt systems.

In conclusion, we believe that the overall errors will be improved after the prototype's integration into the RCD board.

---

<sup>3</sup> Note that LEM LA-150P wasn't tested for the ability to detect a small DC injection and is presented only for a cost comparison.

### **3.6 Future Work**

Going forward, the shunt sensor readout circuitry and the 15VDC dual boost converter PCBs should be integrated into the RCD board in the existing EVSE design.

Next, fine calibration of the sensing system for bidirectional AC current measurements must be performed to reduce bias error to near 0 value. The software would also be updated to respond appropriately to the DC injection information by issuing an error message and opening the safety relay.

Finally, these designs and concepts should be extended to three-phase EVSEs.

### **3.7 Acknowledgement**

The design work presented in this paper was funded by a grant from Nuvve Corp. to the University of Delaware. The authors thank Andrea Wait and Rodney T. McGee from University of Delaware for helpful discussions.

## REFERENCES

- [1] Iec 62053-11:2003, electricity metering equipment (a.c.) - particular requirements - part 11: Electromechanical meters for active energy (classes 0.5, 1 and 2). International standard, International Electrotechnical Commission, 2003.
- [2] American national standard for electricity meters 0.1, 0.2 and 0.5 accuracy classes. Approved american national standard, American National Standards Institute, Inc, 2017.
- [3] DR metering requirements. Technical report, PJM, 06 2018.
- [4] Ieee 1547-2018, ieee standard for interconnection and interoperability of distributed energy resources with associated electric power systems interfaces. Standard, IEEE, 2018.
- [5] Ev meter accuracy testing. Final test report for university of delaware, TESCO ENGINEERING, 2019.
- [6] Monthly Electric Power Industry Report. Technical report, U.S. Energy Information Administration, 01 2020.
- [7] Specifications, tolerances, and other technical requirements for weighing and measuring devices. Standard, National Institute of Standards and Technology Handbook 44, 2020.
- [8] Ahmed Abdelhakim, Paolo Mattavelli, Dongsheng Yang, and Frede Blaabjerg. Coupled-inductor-based dc current measurement technique for transformerless grid-tied inverters. *IEEE Transactions on Power Electronics*, 33(1):18–23, 2018. doi:10.1109/TPEL.2017.2712197.

- [9] Farag Berba, David Atkinson, and Matthew Armstrong. A new approach of prevention of dc current component in transformerless grid-connected pv inverter application. In *Power Electronics for Distributed Generation Systems (PEDG), 2014 IEEE 5th International Symposium on*, pages 1–7. IEEE, 2014. doi:10.1109/PEDG.2014.6878638.
- [10] Marco Crescentini, Marco Marchesi, Aldo Romani, Marco Tartagni, and Pier Andrea Traverso. A broadband, on-chip sensor based on hall effect for current measurements in smart power circuits. *IEEE Transactions on Instrumentation and Measurement*, 67(6):1470–1485, 2018. doi:10.1109/TIM.2018.2795248.
- [11] EKM Metering Inc. *BCT-013-200 Current Transformer Spec Sheet*, 2020.
- [12] Lars Gertmar, Per Karlsson, and Olof Samuelsson. On dc injection to ac grids from distributed generation. In *Power Electronics and Applications, 2005 European Conference on*, pages 10–pp. IEEE, 2005. doi:10.1109/EPE.2005.219420.
- [13] Willett Kempton and Jasna Tomić. Vehicle-to-grid power fundamentals: Calculating capacity and net revenue. *Journal of power sources*, 144(1):268–279, 2005. doi:10.1016/j.jpowsour.2004.12.025.
- [14] Francis Laurent A. and Krzysztof Iniewski. Novel advances in microsystems technologies and their applications. *CRC Press, TaylorFrancis Group*, pages 266–287, 2016.
- [15] Maria Gabriella Masi, Lorenzo Peretto, and Roberto Tinarelli. Design and performance analysis of a differential current sensor for power system applications. *IEEE Transactions on Instrumentation and Measurement*, 61(12):3207–3215, 2012. doi:10.1109/TIM.2012.2205513.
- [16] Olga Mironenko, Willett Kempton, and Fouad Kiamilev. Dc injection from electric vehicles and possible solutions: A review. *Ready for a journal submission*, April 2020.

- [17] Carlo Muscas, Marco Pau, Paolo Attilio Pegoraro, and Sara Sulis. Smart electric energy measurements in power distribution grids. *IEEE Instrumentation & Measurement Magazine*, 18(1):17–21, 2015. doi:10.1109/MIM.2015.7016676.
- [18] Gert Rietveld, Jean-Pierre Braun, Ricardo Martin, Paul Wright, Wiebke Heins, Nikola Ell, Paul Clarkson, and Norbert Zisky. Measurement infrastructure to support the reliable operation of smart electrical grids. *IEEE Transactions on Instrumentation and Measurement*, 64(6):1355–1363, 2015. doi:10.1109/TIM.2015.2406056.
- [19] Pavel Ripka. Electric current sensors: a review. *Measurement Science and Technology*, 21(11):112001, 2010. doi:10.1088/0957-0233/21/11/112001.
- [20] Chucheng Xiao, Lingyin Zhao, Tadashi Asada, WG Odendaal, and JD Van Wyk. An overview of integratable current sensor technologies. In *Industry Applications Conference, 2003. 38th IAS Annual Meeting. Conference Record of the*, volume 2, pages 1251–1258. IEEE, 2003. doi:10.1109/IAS.2003.1257710.
- [21] Weichi Zhang, Matthew Armstrong, and Mohammed Elgendy. Dc current determination in grid-connected transformerless inverter systems using a dc link sensing technique. In *Energy Conversion Congress and Exposition (ECCE), 2017 IEEE*, pages 5775–5782. IEEE, 2017. doi:10.1109/ECCE.2017.8096958.
- [22] Silvio Ziegler, Robert C Woodward, Herbert Ho-Ching Iu, and Lawrence J Borle. Current sensing techniques: A review. *IEEE Sensors Journal*, 9(4):354–376, 2009. doi:10.1109/JSEN.2009.2013914.
- [23] A. F. Zobaa and C. Cecati. A comprehensive review on distributed power generation. *International Symposium on Power Electronics, Electrical Drives, Automation and Motion. SPEEDAM*, 2006. doi: 10.1109/SPEEDAM.2006.1649826.

## Chapter 4

### COMPARING DEVICES FOR CONCURRENT MEASUREMENT OF AC CURRENT AND DC INJECTION FOR ELECTRIC VEHICLE CHARGING

*In Chapter 3, a shunt-based AC and DC current sensing system for single-phase EVSEs has been designed, prototyped, and tested. The prototype can simultaneously conduct high precision revenue metering and detect DC injection into the grid by EV's on-board equipment in case of a fault. In addition, the new system is capable of interconnection with any EV. Chapter 4 represents the third study where we compare performance and cost of the designed system with the current sensing system (CT) commonly used in EVSE as well as with other top candidate namely the fluxgate current sensor. First, we introduce the structure, capabilities and limitations of each system. Further, we provide the accuracy and the cost of each system under interest. Finally, we compare the systems based on capabilities to measure both AC current up to 80 A with high precision and detect the DC injection of  $\geq 400$  mA along with the cost of each system. In conclusion, we provide a recommendation for the optimal solution to be used in bidirectional 19.2 kW single-phase EVSEs.*

#### 4.1 Abstract

Widespread adoption of electric vehicles (EVs) requires additional safety countermeasures to prevent DC injection from EVs into the AC grid via Electric Vehicle Supply Equipment (EVSE). Moreover, for energy purchase, and even more so for vehicle-to-grid (V2G) services, the EVSE must conduct high precision bidirectional power and energy measurements. The paper introduces operating principles, structure, performance and cost comparison of three current sensing technologies—current

transformer, shunt and fluxgate—for metering and protection within an EVSE, concluding with recommendations among those sensors for the most beneficial applications concerning EV charging.

## 4.2 Introduction

Any faulty power converter can inject some portion of DC current into the AC grid. This effect is called "DC injection". Acceptable level of DC injection is specified in "Limitation of DC injection" section of IEEE 1547-2018 standard [4]. The level of DC injection above 0.5% of the full rated output current can cause various negative effects to other grid equipment [7, 17]. It is especially important for high power converters such as employed in electric vehicles (EVs). Therefore, this article recommends that the level of DC injection from EVs should be monitored via electric vehicle supply equipment (EVSE) as a gateway between the grid and EV's power converters. A separate check in the EVSE would be an economically efficient way to ensure grid safety[13, 12]. Due to regulatory officials being especially concerned about bidirectional charging, verification of DC injection for Vehicle-to-Grid technology (V2G), which enables the bidirectional power flow between the electric vehicle (EV) batteries and the grid, may be considered especially important [12, 8].

The EVSE governs the connection of grid power to the vehicle power converter, and thus is a major part of any EV system. Some EVSE's are capable of measuring both the instantaneous power flow and the accumulated kWh of energy consumed. The measurement may be required for EVSE working in conjunction with grid measurements such as controlled charging. Furthermore, V2G capable EVSE can allow conducting power back to the grid, and thus the metering must be bidirectional. It would be expected to be cost-efficient to use the same device to measure both the AC charging power and the DC injection. However, the two orders of magnitude differences of measured AC vs. DC currents makes using the same instrument challenging. Fortunately, it is the much larger AC quantities that require greater accuracy.

The accuracy criteria for power and energy and, consequently, AC current measurements for revenue meters (so-called "revenue grade" accuracy) are defined in NIST HB-44, ANSI C12.20 and IEC 62053-11 standards (0.5, 1.0 and 2.0 accuracy classes) [5, 2, 1]. A meter will satisfy the majority of regional transmission operators (RTOs) in North America and Europe, if the meter is able to meet all three accuracy classes. However, U.S. markets such as PJM are satisfied with meter's performance within 1.0 or 2.0 accuracy classes [3].

The system requirements for the current sensing system inside the V2G capable EVSE are summarized in a Table 4.1.

**Table 4.1:** Current metering system requirements for single-phase and for three-phase EVSEs.

Parameters	Requirements	
	Single phase unit (19.2 kW)	Three phase unit (100 kW)
Voltage (L-N)	120V, 230V	120V, 230V, 277V, 347V
DC injection limit	0.5% of $I_{rated}$	
DC injection detection accuracy at the limit value	10%-20%	
AC current metering accuracy classes	0.5, 1.0, 2.0	
$I_{rated}$	80A	120A
Cost	Low	

The system must obey the standards for AC revenue metering accuracy and for DC injection limitation (see 4.2). Note that "Limitation of DC injection" section of IEEE 1547-2018 standard doesn't specify an accuracy of DC injection detection. Rather, the designer must establish sufficient accuracy that the measured value will be very likely no more than the required threshold value. The authors estimate a safe tolerance to be 10%-20% of the limit value.

In addition, the system must satisfy the AC current range of  $I_{rated}$  as well as must be compatible with electrical systems worldwide (as much as practical). Finally, the last important criteria is a low system's cost [12].

This paper compares operating principles, performance and cost<sup>1</sup> of three current sensing systems: current transformer (CT), shunt, and fluxgate for single-phase and three-phase EVSE in application of high precision AC revenue metering and DC injection detection. In addition, the paper recommends the most optimal solution for concurrent revenue metering and DC injection detection according to the system requirements listed in a Table 4.1 as well as possible EV charging applications for other two systems.

### 4.3 Current Transformer Current Sensing System

#### 4.3.1 Operating principle

The most common AC current sensing system for revenue-grade metering utilizes a current transformer (CT). Since it is based on Faraday's Law of induction, CT can only detect the AC current, it is blind to DC injection.

A CT consists of a ferrite core and primary and secondary windings coupled together so that the induced current in the secondary coil is proportional to the primary current. The former can be calculated from the induced current using the known windings turn ratio. In power measurement devices, the primary "winding" is typically the main current-carrying wire passing through once or looped a few times around the CT coil containing the secondary winding (see Fig. 4.1).

CTs are popular for revenue-grade metering systems due to their high accuracy, low complexity, and isolation. In addition, CTs are directly compatible with analog-to-digital converters. However, high accuracy CTs can be costly, as they employ high relative permeability core materials [13, 18, 9, 14].

---

<sup>1</sup> Prices are collected from Digi-Key Electronics, Mouser Electronics, Vango Technology, KG Technologies and Magnetic Sensor Systems (estimate for 1000+ quantity). Parts price below \$0.5 is not included.

### 4.3.2 System structure and capabilities

The CT current sensing system (Fig. 4.1) was designed and developed at the University of Delaware by the V2G research group. The UD-developed system is currently in use for high precision AC current, voltage and power measurements in EVSE commercial units.

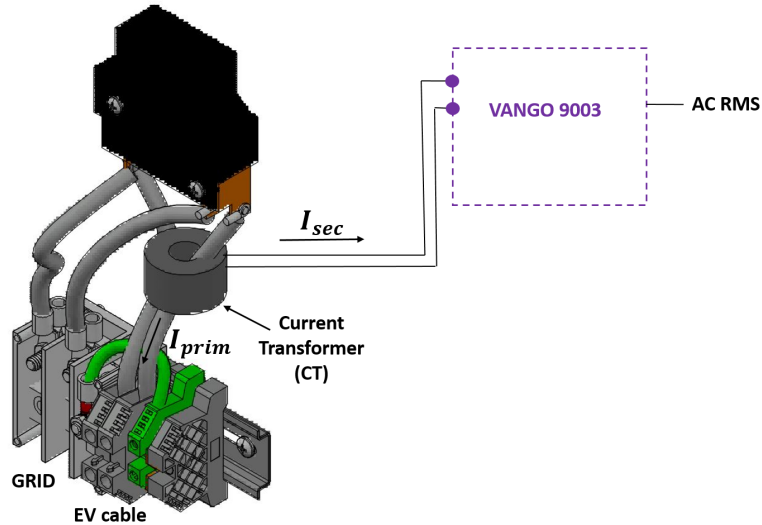


**Figure 4.1:** Current transformer current sensing system for a single-phase EVSE

The system consists of the BCT-013-200 CT,  $\pm 0.1\%$  precision resistor network and the Vango 9003 metrology chip, used in many submeters. The CT is placed around the main current conductor, and the other elements are integrated into a circuit board.

The current to be measured  $I_{prim}$  is picked up by CT. Secondary current  $I_{sec}$ , proportional to  $I_{prim}$ , is induced and processed through the metrology chip, where the current RMS value is calculated. The system is specified to measure AC currents up to 200 A.

The main disadvantage of the system is its incapability to detect DC currents (see 4.3.1). Moreover, the CT system becomes very inaccurate at currents below 6A.

### 4.3.3 Accuracy

The manufacturer guarantees the BCT-013-200 CT is  $\pm 0.1\%$  accuracy. Therefore, the calibration of each EVSE unit is not required, which simplifies the EVSE manufacturing process. The overall CT sensing system has been measured and certified by TESCO Engineering to 1.0 accuracy class.

### 4.3.4 Cost

The detailed cost of the single and three-phase systems is shown in Table 4.2.

**Table 4.2:** Current transformer current sensing system: detailed cost for single and three-phase EVSE. Hall-Effect LEM sensor is added only for DC injection detection price estimate.

Single-phase system			Three-phase system	
Part No	Qty	Price	Qty	Price
BCT-013-200 CT	1	\$14	3	\$42
Vango 9003	1	\$3.15	1	\$3.15
LEM LA-150P	1	\$19.04	3	\$57.12
LT1945EMS	1	\$2.60	1	\$2.60
<b>Approximate total cost</b>		\$38.79	\$104.87	

As we mentioned in 4.3.2, the CT current sensing system is only capable to detect AC current. Therefore, the separate DC current sensor must be installed to extend the measurement range to DC currents. Authors selected a closed-loop Hall-Effect current sensor LEM LA 150-P with operating range up to 150 A and 0.5% accuracy at the primary nominal current of 150 A. In addition, the price of dual power supply LT1945EMS, required for the sensor, was included in the cost estimate.

The closed-loop Hall Effect sensor belongs to magnetic sensors family and is capable of measuring AC and DC signals. The sensor's operating principle is based on Hall Effect when the Lorenz force affects the charged particle moving in the presence of a magnetic field.

The closed-loop Hall Effect sensor concentrates the magnetic field created by the current to be measured in a magnetic core surrounding the main conductor. This

magnetic field is measured through the Hall voltage. The output Hall voltage is converted to the secondary current which is proportional to the current under interest [11, 6, 13].

Note that the Hall-Effect sensor was not tested for the ability to detect 400 mA DC injection; it is presented here for the price comparison, not necessarily as a technology ready for this purpose. In addition, it is important to mention, that authors don't include a Hall-Effect current sensor as a stand alone solution for the application of interest due to its lack of standards-required accuracy at low currents.

## **4.4 Shunt Current Sensing System**

### **4.4.1 Operating principle**

A shunt is based on Ohm's Law of resistance and thus is capable of measuring both AC and DC currents. The measured voltage drop across the shunt is proportional to the current flowing through it. A shunt is a simple, low-cost current sensing solution with an acceptable level of accuracy. Typical measuring accuracy of a shunt is  $\pm 0.1\%$ ,  $\pm 0.25\%$ , or  $\pm 0.5\%$ . Drawbacks of shunt current sensors are (1) the absence of galvanic isolation, (2) the heat release due to power dissipation on a resistor, and (3) the weak output signal due to a voltage drop in several mV ranges, requiring signal amplification [12, 13].

### **4.4.2 System structure and capabilities**

The shunt current sensing system prototype was also designed and developed by the University of Delaware V2G research group [12]. The prototype system structure is shown in Fig. 4.2.

The system consists of a single shunt current sensor and two readout circuits (AC and DC). The shunt is installed into a latching safety relay lead inside the EVSE. The current to be measured generates a voltage drop across the shunt. The voltage drop is picked up by readout circuits and processed by Vango 9003 metrology chip.

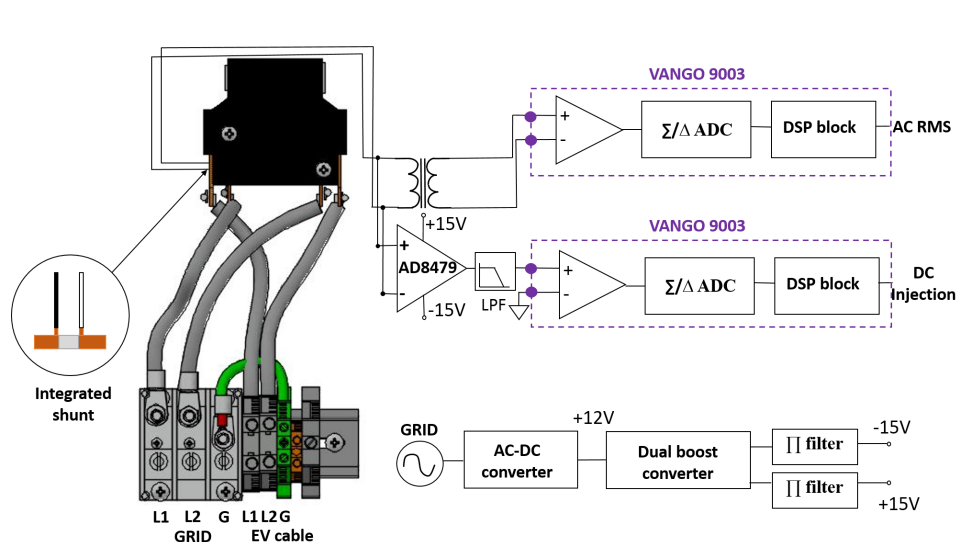


**Figure 4.2:** Current sensing single phase system block diagram.

The circuit on the top is responsible for high precision AC current measurements, whereas the circuit underneath is dedicated to DC injection detection. In order to determine whether the DC injection value is above the safe limit or not, Vango 9003 splits the bottom analog circuit's AC+DC mixed output signal by its components and calculates the DC injection.

The system is verified to be linear for AC current from 6 A to 35 A, and has a potential to extend the linear range to 80 A. In addition, it can simultaneously detect DC injection of 400 mA or more in an AC signals up to 80 A. However, the system has been tested only for a 19.2 kW single-phase EVSE, it has a potential to be extended to a 100 kW three-phase EVSE.

Note that in the next design revision, all the components will be integrated into the main printed circuit board (PCB), but due to time and fabrication cost constrains, the prototype presented in this paper is designed on a separate PCB board connected to the main one.

### 4.4.3 Accuracy

For AC current revenue metering the system meets 1.0 accuracy class requirements defined in NIST HB-44 when charging (power flows from the grid to an EV) and when discharging (power flows from an EV to the grid).

The accuracy of DC injection detection at the limit value of 400 mA is 8.25% when DC injection is positive, and the accuracy is 16.5% when DC injection is negative. Moreover, we believe, that more precise calibration and the prototype integration into the main PCB will result in further accuracy improvement.

Although the shunt current sensing system fulfills the requirements listed in Table 4.1, calibration of each EVSE unit is essential due to  $\pm 5\%$  shunt tolerance. In addition, further work is required to integrate the prototype into commercial EVSE production.

### 4.4.4 Cost

The cost of the system is shown in Table 4.3.

**Table 4.3:** Shunt current sensing system: detailed cost for single and three-phase EVSE.

Single-phase system			Three-phase system	
Part No	Qty	Price	Qty	Price
Shunt	1	\$3	3	\$5
Vango 9003	1	\$3.15	1	\$3.15
TTC-5036	1	\$2.52	3	\$7.56
AD8479ARZ-RL	1	\$4.25	3	\$12.75
LT1945EMS	1	\$2.60	1	\$2.60
<b>Approximate total cost</b>		<b>\$15.52</b>		<b>\$31.06</b>

Table 4.3 lists prices for the major parts of the system. In addition to shunt sensor and Vango 9003 metrology chip, authors included prices for the signal transformer TTC-5036 utilized in AC readout circuit, operational amplifier AD8479ARZ-RL utilized in DC readout circuit and DC/DC converter LT1945EMS utilized in dual boost converter (Fig. 4.2).

## 4.5 Fluxgate Current Sensing System

### 4.5.1 Operating principle

Fluxgate current sensors are magnetic field sensors that can detect low-frequency AC and DC currents, in contrast to CT. Fluxgate utilizes a non-linear relation between the ferromagnetic material permeability and the ambient magnetic field.

The basic fluxgate sensor consists of a ferromagnetic rod-shaped core, an excitation coil, and a pick-up coil. The high-frequency excitation signal is sent through the excitation winding to drive the core to saturation in both directions. At the moment of core saturation, a significant reduction in its magnetic permeability occurs, causing the ambient magnetic flux to collapse. The magnetic flux change induces a measurable voltage in the pick-up coil, which is proportional to the ambient magnetic field. The Fluxgate sensor's name derives from the magnetic flux "gating" effect at the saturation point. Although fluxgate is one of the most accurate magnetic sensors (up to  $\pm 0.0002\%$ ), their application is limited due to its complexity and high price [13, 10, 15].

### 4.5.2 System structure and capabilities

The Fluxgate current sensing system prototype was developed by Magnetic Sensor Systems LLC [16]. The system consists of a fluxgate sensor head, placed around a copper conductor, and a controller board. The controller board has excitation and readout circuits for a sensor head.

The current to be measured flows through the conductor, generating a magnetic flux picked up by a sensor head, and processed by a controller board (Fig.4.3).

Due to its nature, the fluxgate sensor current sensing system is capable of conducting both AC measurements and DC injection detection. The system is able to measure AC and DC currents in the range of  $\pm 50$  A. In addition, the fluxgate sensor head is highly consistent across several production units. Therefore, no calibration per unit is required in serial production.

Note that the system has been tested at the minimum current of 1 A. Therefore, further testing is required to conclude on the sensor's ability to detect DC injection

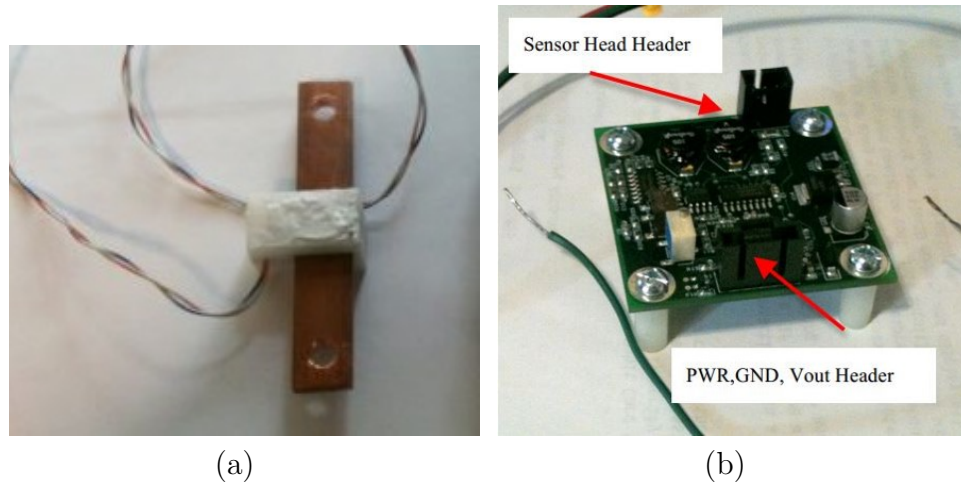


**Figure 4.3:** Fluxgate current sensing system's prototype: (a) The sensor head. (b) Controller board (images used by permission of Magnetic Sensor Systems, LLC).

$\geq 400$  mA. In addition, as it has been mentioned above, the Fluxgate current sensing system is on a prototype stage, and further design work is needed to incorporate the current sensing system into any production device, such as an EVSE.

#### 4.5.3 Accuracy

Accuracy data for DC currents is provided by Magnetic Sensor Systems LLC [16]. For positive currents, the system demonstrates the accuracy about 0.1% of full scale (FS) for currents up to 30 A. However, accuracy is lower at higher currents, where the accuracy is 1.2% of FS near 50 A. For negative currents, the system is accurate to approximately 0.3% of FS.

#### 4.5.4 Cost

The detailed cost of the system is shown in Table 4.4.

The cost estimate for each part of the fluxgate sensing system is provided by Jeff Viola, Magnetic Sensor Systems LLC.<sup>2</sup> Note that Vango 9003 metering chip is included only to estimate the approximate cost of the sensor's output signal processing.

---

<sup>2</sup> Email from 10/17/2019, Jeff Viola, MSS llc, jeff@magsensorsystems.com

**Table 4.4:** Fluxgate current sensing system: detailed cost for single and three-phase EVSE

Single-phase system			Three-phase system	
Part No	Qty	Price	Qty	Price
Fluxgate sensor head	1	\$0.57	3	\$1.71
Controller board	1	\$14.85	3	\$44.55
Vango 9003	1	\$3.15	1	\$3.15
<b>Approximate total cost</b>		\$18.57	\$49.41	

#### 4.6 Systems comparison and recommended applications

The comparison of aforementioned systems is presented in Table 4.5.

**Table 4.5:** Comparison of three current sensing systems for single-phase and three-phase EVSEs

Characteristics	CT + Hall Effect	Fluxgate	Shunt
System complexity	low	high	moderate
Operating current range	200 A	$\pm 50$ A	35 A (verified) 80 A (in progress)
Operating voltage range	Isolated	Isolated	600 V
AC revenue metering accuracy class (0.5,1.0,2.0):	1.0	N/A	1.0
DC accuracy (@ 400 mA):			
Positive	N/A	N/A	8.25%
Negative	N/A	N/A	16.5%
Calibration/unit	not required	not required	required
Total cost, single phase EVSE	\$38.79	\$18.57	\$15.52
Total cost, three phase EVSE	\$104.87	\$49.41	\$31.06

A CT current sensing system can be successfully used as a simple and inexpensive device for high precision revenue metering inside the EVSE. However, the DC current is invisible for CT. Therefore, the CT system can not be employed for DC injection detection without an additional DC current sensor. Consequently, overall cost of the system will increase approximately twice.

In contrast, Fluxgate current sensing system is capable of detecting DC current, but the system has not been tested at the currents below 1 A. Therefore, further testing is required to evaluate the sensor's ability to detect DC injection with required accuracy. In addition, the system has limited operating current range. Therefore, we do not

recommend the system at its current state for a single-phase or a three-phase V2G EVSEs, specified in a Table 4.1.

The shunt current sensing system can detect DC injection within the EVSE system requirements (Table 4.1) and conduct bidirectional AC current measurements with acceptable accuracy for 19.2 kW single-phase EVSE. The authors have verified accuracy only up to 35 A, the shunt system is believed able to extend the measurement range up to 80 A single-phase or 120 A three-phase EVSE. Therefore, the shunt sensing system holds promise for V2G capable as well as regular EVSE applications. Although the system is currently on a prototype stage, we believe that it can be successfully incorporated into EVSE units for commercial production.

#### **4.7 Conclusions**

In this work, we compared operating principles, structure, performance and the cost of CT, fluxgate and shunt current monitoring systems for concurrent AC revenue metering and DC injection measurements for EV charging and discharging. We described advantages and weaknesses of each system, and provided a recommendation for their most beneficial applications with EV charging. The shunt current sensing system was recommended as the best suited for simultaneous detection of DC injection and accurate AC revenue metering.

#### **4.8 Acknowledgement**

The work presented in this paper was funded by a grant from Nuvve Corp. to the University of Delaware.

## REFERENCES

- [1] Iec 62053-11:2003, electricity metering equipment (a.c.) - particular requirements - part 11: Electromechanical meters for active energy (classes 0.5, 1 and 2). International standard, International Electrotechnical Commission, 2003.
- [2] American national standard for electricity meters 0.1, 0.2 and 0.5 accuracy classes. Approved american national standard, American National Standards Institute, Inc, 2017.
- [3] DR metering requirements. Technical report, PJM, 06 2018.
- [4] Ieee 1547-2018, ieee standard for interconnection and interoperability of distributed energy resources with associated electric power systems interfaces. Standard, IEEE, 2018.
- [5] Specifications, tolerances, and other technical requirements for weighing and measuring devices. Standard, National Institute of Standards and Technology Handbook 44, 2020.
- [6] Loredana Cristaldi, Alessandro Ferrero, Massimo Lazzaroni, and RT Ottoni. A linearization method for commercial hall-effect current transducers. *IEEE transactions on Instrumentation and Measurement*, 50(5):1149–1153, 2001. doi:10.1109/19.963175.
- [7] Lars Gertmar, Per Karlsson, and Olof Samuelsson. On dc injection to ac grids from distributed generation. In *Power Electronics and Applications, 2005 European Conference on*, pages 10–pp. IEEE, 2005. doi:10.1109/EPE.2005.219420.

- [8] Willett Kempton and Jasna Tomić. Vehicle-to-grid power fundamentals: Calculating capacity and net revenue. *Journal of power sources*, 144(1):268–279, 2005. doi:10.1016/j.jpowsour.2004.12.025.
- [9] William Koon. Current sensing for energy metering. In *Conference Proceedings IIC-China/ESC-China*, pages 321–324, 2002.
- [10] Francis Laurent A. and Krzysztof Iniewski. *Novel Advances in Microsystems Technologies and Their Applications*. CRC Press, TaylorFrancis Group, 2016.
- [11] James E Lenz. A review of magnetic sensors. *Proceedings of the IEEE*, 78(6):973–989, 1990. doi:10.1109/5.56910.
- [12] Olga Mironenko, Garrett Ejzak, Willett Kempton, and Fouad Kiamilev. Integrated electric vehicle shunt current sensing system for concurrent revenue metering and detection of dc injection. *re-submitted to IEEE transactions on Instrumentation and Measurement*, June 2020.
- [13] Olga Mironenko, Willett Kempton, and Fouad Kiamilev. Current sensing techniques for revenue metering and detection of direct current injection from electric vehicles: A review. *submitted to SAE International Journal of Electrified Vehicles*, May 2020.
- [14] Louie J Powell. Current transformer burden and saturation. *IEEE Transactions on Industry Applications*, (3):294–303, 1979. doi:10.1109/TIA.1979.4503656.
- [15] Pavel Ripka. Advances in fluxgate sensors. *Sensors and Actuators A: Physical*, 106(1-3):8–14, 2003. doi:10.1016/S0924-4247(03)00094-3.
- [16] Jeff Viola. Fluxgate Current Sensor m-3 Deliverable Document. Technical report, Magnetic Sensor Systems, 09 2010.

- [17] Wei Wang, Ping Wang, Taizhou Bei, and Mengmeng Cai. Dc injection control for grid-connected single-phase inverters based on virtual capacitor. *Journal of Power Electronics*, 15(5):1338–1347, 2015. doi:10.6113/JPE.2015.15.5.133.
- [18] Silvio Ziegler, Robert C Woodward, Herbert Ho-Ching Iu, and Lawrence J Borle. Current sensing techniques: A review. *IEEE Sensors Journal*, 9(4):354–376, 2009. doi:10.1109/JSEN.2009.2013914.

## CONCLUSIONS

The three studies presented here have proposed a cost-effective solution for the problem of DC injection. More concretely, chapter 2 investigated the historical roots of the DC injection problem and existing studies on DC injection mitigation as well as its relation to EV charging and discharging. Furthermore, chapter 2 explained the necessity to design a new cost-effective current sensing system for DC injection detection combined with high precision AC current measurements to be used in uni and bidirectional EVSEs as an extra safety measure to ensure power quality. The main contribution of the study is under new design requirements for V2G EVs, and to develop and test appropriate product for the next design steps by specifying several current sensing technologies, suitable for the application in question, from wide range of current sensing techniques available on the market. In addition, the study can help other engineers in automotive industry to make a decision about the appropriate product for current sensing.

The chapter 3 introduced the integrated shunt current sensing system we designed. The chapter described the design challenges, the prototype and test results for DC injection detection and AC current measurement accuracy. The designed system accomplishes DC injection detection along with high precision AC current measurement through the single sensing element. It makes the new system to be cost-effective over the common EVSE current sensing system which is important considering mass production of EVSE. More detailed, the system meets 1.0 accuracy class requirements for currents from 6 A to 35 A. We believe, the accuracy will be improved after the prototype's integration into the main EVSE system. The design contributes in the field of EVs and the grid as well as other current sensor applications such as battery management systems.

Finally, chapter 4 compared the structure, performance, limitations and cost of the current sensing system designed in chapter 3 with the common current sensing system for EVSE (current transducer) and with the other top candidate selected in the chapter 2, namely fluxgate current sensing systems. Furthermore, chapter 4 provided the recommendation of the most beneficial system for EV charging application. The integrated shunt current sensing system was recommended as the optimal solution for simultaneous DC injection detection and high precision AC current measurement for bidirectional EV charging. As the main chapter 4 contribution, the study will help engineers from this project, as well as other EVSE designers, to select the proper system for various current sensing applications in EVSEs not only based on technical criteria but also based on systems' cost-effectiveness.

In sum, the aforementioned contributions improve the grid safety in a cost-efficient way for unidirectional and bidirectional EV charging. Considering the rapid growth of the electric automotive industry, such improvement would be very beneficial to the field of renewable energy integration.